







# Therapeutically useful mycobacteriophages BPs and Muddy require trehalose polyphleates

Received: 14 March 2023

Accepted: 17 July 2023

Published online: 24 August 2023

 Check for updates

Katherine S. Wetzel <sup>1,5</sup>, Morgane Illouz <sup>2,5</sup>, Lawrence Abad<sup>1</sup>, Haley G. Aull<sup>1</sup>, Daniel A. Russell <sup>1</sup>, Rebecca A. Garlena<sup>1</sup>, Madison Cristinziano<sup>1</sup>, Silke Malmshaimer<sup>2</sup>, Christian Chalut <sup>3</sup>, Graham F. Hatfull <sup>1</sup> ✉ & Laurent Kremer <sup>2,4</sup> ✉

Mycobacteriophages show promise as therapeutic agents for non-tuberculous mycobacterium infections. However, little is known about phage recognition of *Mycobacterium* cell surfaces or mechanisms of phage resistance. We show here that trehalose polyphleates (TPPs)—high-molecular-weight, surface-exposed glycolipids found in some mycobacterial species—are required for infection of *Mycobacterium abscessus* and *Mycobacterium smegmatis* by clinically useful phages BPs and Muddy. TPP loss leads to defects in adsorption and infection and confers resistance. Transposon mutagenesis shows that TPP disruption is the primary mechanism for phage resistance. Spontaneous phage resistance occurs through TPP loss by mutation, and some *M. abscessus* clinical isolates are naturally phage-insensitive due to TPP synthesis gene mutations. Both BPs and Muddy become TPP-independent through single amino acid substitutions in their tail spike proteins, and *M. abscessus* mutants resistant to TPP-independent phages reveal additional resistance mechanisms. Clinical use of BPs and Muddy TPP-independent mutants should preempt phage resistance caused by TPP loss.

Non-tuberculous mycobacteria include several important human pathogens such as *Mycobacterium abscessus* and *M. avium*<sup>1,2</sup>. These infections are often refractory to effective antibiotic treatment due to both intrinsic and acquired resistance mutations, and new treatment options are needed<sup>3</sup>. The therapeutic application of mycobacteriophages shows some promise for the treatment of pulmonary infections in persons with cystic fibrosis<sup>4–6</sup>, disseminated infection following bilateral lung transplantation<sup>4</sup> and disseminated *M. chelonae* infection<sup>7</sup>. However, broadening therapy beyond single-patient compassionate use applications will require expansion of the repertoire of therapeutically useful

phages and increasing host range such that a higher proportion of clinical isolates can be treated<sup>5,8,9</sup>. Clinical administration of bacteriophages is anticipated to give rise to phage-resistant mutants and disease recurrence<sup>10</sup>, but the frequency and mechanisms of mycobacteriophage resistance are poorly understood<sup>11</sup>. Very few mycobacteriophage receptors are known, although glycopeptidolipids (GPLs) are proposed as receptors for mycobacteriophage I3 in *M. smegmatis*<sup>12</sup>.

Over 12,000 individual mycobacteriophages have been described, with most having been isolated on *M. smegmatis*<sup>13</sup>. The genome sequences of 2,200 of these show them to be highly diverse genetically

<sup>1</sup>Department of Biological Sciences, University of Pittsburgh, Pittsburgh, PA, USA. <sup>2</sup>Centre National de la Recherche Scientifique UMR 9004, Institut de Recherche en Infectiologie de Montpellier (IRIM), Université de Montpellier, Montpellier, France. <sup>3</sup>Institut de Pharmacologie et de Biologie Structurale, Université de Toulouse, CNRS, UPS, Toulouse, France. <sup>4</sup>INSERM, IRIM, Montpellier, France. <sup>5</sup>These authors contributed equally: Katherine S. Wetzel, Morgane Illouz. ✉e-mail: [gfh@pitt.edu](mailto:gfh@pitt.edu); [laurent.kremer@irim.cnrs.fr](mailto:laurent.kremer@irim.cnrs.fr)

and pervasively mosaic<sup>14,15</sup>. They can be sorted into groups of genomically related phages (for example, Cluster A, B, C and so on), some of which can be readily divided into subclusters (for example, Subcluster A1, A2, A3 and so on) on the basis of sequence variation<sup>16,17</sup>. Seven of the sequenced phages currently have no close relatives and are designated as ‘singletons’<sup>18</sup>. A subset of these phages have relatively broad host range and are also able to efficiently infect *M. tuberculosis*, including phages in Clusters/Subclusters A2, A3, G1, K1, K2, K3, K4 and AB<sup>19,20</sup>. A similar subset of phages also infect some clinical isolates of *M. abscessus*, although it is noteworthy that phage host ranges on these strains are highly variable (even for related phages within clusters/subclusters) and are highly variable among different clinical isolates<sup>4,9</sup>. There is also substantial variation in the outcomes of phage infection of *M. abscessus* strains, with notable differences between rough and smooth colony morphotypes<sup>9</sup>. For example, a smaller proportion of smooth isolates are susceptible to phage infection compared with rough strains, as determined by plaque formation, and none of the smooth strains is efficiently killed by any phage tested<sup>9</sup>.

Mycobacterial cell walls characteristically have a mycolic acid-rich outer layer referred to as the mycobacterial outer membrane or mycomembrane<sup>21</sup>. In addition to abundant mycolic acids, there are numerous other types of complex molecule including multiple acylated lipids such as di- and polyacyltrehalose (DAT and PAT), phthiocerol dimycocerosate and sulfoglycolipids, although not all are found in all *Mycobacterium* species. Smooth strains of *M. abscessus* have abundant GPLs, whereas these are lacking or greatly less abundant in rough strains<sup>22,23</sup>. Recently, it has been shown that some mycobacterial species, including *M. abscessus*, have trehalose polyphosphates (TPPs), which are high-molecular-weight, surface-exposed glycolipids, in their cell walls<sup>24,25</sup>. These TPPs may be important for *M. abscessus* virulence and are associated with clumping and cording<sup>25</sup>. A five-gene cluster, including a polyketide synthetase (Pks), is required for TPP biosynthesis and TPP precursor (DAT) transport to the outer surface of the cell by MmpL10 (ref. 26). TPPs are not present in *M. tuberculosis* although DAT and PAT are<sup>26</sup>. The specific roles of TPPs are not known, but their position on the outer surface makes them candidates for use as phage receptors.

Here we show that TPPs are required for the binding and infection of *M. abscessus* by phages BPs and Muddy. These phages share little or no nucleotide similarity but both have been used therapeutically, sometimes in combination with each other<sup>4,27</sup>. *M. abscessus* transposon insertion mutants that are resistant to these phages map in all five genes involved in TPP synthesis, all have lost TPPs from their cell walls and phage adsorption is lost. Spontaneous phage-resistant mutants of some *M. abscessus* clinical isolates also have mutations in the known TPP synthesis genes, and some *M. abscessus* clinical isolates that are insensitive to BPs and Muddy are naturally defective in TPPs. However, the TPP requirement can be readily overcome by mutations in phage

tail spike proteins, suggesting that TPPs are acting as a co-receptor, and the cell wall binding target of the phages is probably essential for mycobacterial viability. *M. abscessus* strains resistant to BPs and Muddy TPP-independent mutants reveal new mechanisms of phage resistance.

## Results

### Transposon mutagenesis of *M. abscessus* clinical isolates

*M. abscessus* GD01 (subspecies *massiliense*) was selected for transposon mutagenesis as it is the first clinical isolate treated therapeutically<sup>4</sup> and is killed well by phages Muddy, ZojΔ45 and BPsΔ33HTH\_HRM10, mapping in Clusters AB, K2 and G1, respectively. Muddy is a lytic phage and ZojΔ45 and BPsΔ33HTH\_HRM10 are engineered lytic derivatives of Zoj<sup>28</sup> and BPs<sup>29</sup>, respectively. Because GD01, similar to many *M. abscessus* isolates, is kanamycin resistant (minimum inhibitory concentration (MIC) > 128 μg ml<sup>-1</sup>)<sup>30</sup>, we re-engineered the extant Kan<sup>R</sup> MycoMarT7 transposon using CRISPY-BRED<sup>31</sup> to include an Hyg<sup>R</sup> cassette, constructing derivatives both with and without the existing R6Kγ origin of replication (Fig. 1a). The shorter transposon (MycoMarT7-Hyg2) transduced strain GD01-100 times more efficiently than the longer MycoMarT7-Hyg1 transposon; this efficiency difference was not observed for *M. smegmatis*. We transduced strain GD01 with MycoMarT7-Hyg2 and selected Hyg-resistant transductants on solid media to yield a random mutagenesis library (Fig. 1b). We note that the parent of the transposon delivery phages, TM4, does not form plaques on any *M. abscessus* strain<sup>9</sup> but efficiently delivers DNA to *M. abscessus* cells<sup>32</sup>.

### Phage-resistant mutants are defective in TPPs

To identify *M. abscessus* GD01 phage-resistant mutants, the Tn library was plated on solid media seeded with either BPsΔ33HTH\_HRM10 or Muddy. Single colonies were recovered at a frequency of ~10<sup>-3</sup> and 20 individual colonies were picked from each selection, rescreened and characterized (Fig. 1, Extended Data Fig. 1 and Extended Data Table 1). Eighteen of the 20 BPsΔ33HTH\_HRM10-resistant candidates were mapped, all of which have transposon insertions in a gene cluster involved in TPP synthesis; some appear to have secondary transposon insertions mapping elsewhere (Extended Data Table 1 and Fig. 1c,d). Thirteen of the 20 Muddy resistant candidates were mapped and surprisingly, all also contain insertions in TPP synthesis genes (Extended Data Table 1 and Fig. 1c,d). TPP synthesis has previously been reported to be non-essential<sup>33</sup> and these observations suggest that loss of TPPs is the primary mechanism of resistance to both BPsΔ33HTH\_HRM10 and Muddy. Further analysis showed that all of the mutants tested have similar phenotypes, with a large reduction in the efficiency of plaquing of BPsΔ33HTH\_HRM10 and a more modest reduction in the efficiency of plaquing of Muddy, but with formation of very turbid plaques (Fig. 1e). Complementation of a *fadD23* Tn mutant confirmed that phage resistance results from TPP loss (Fig. 1f). All of the strains

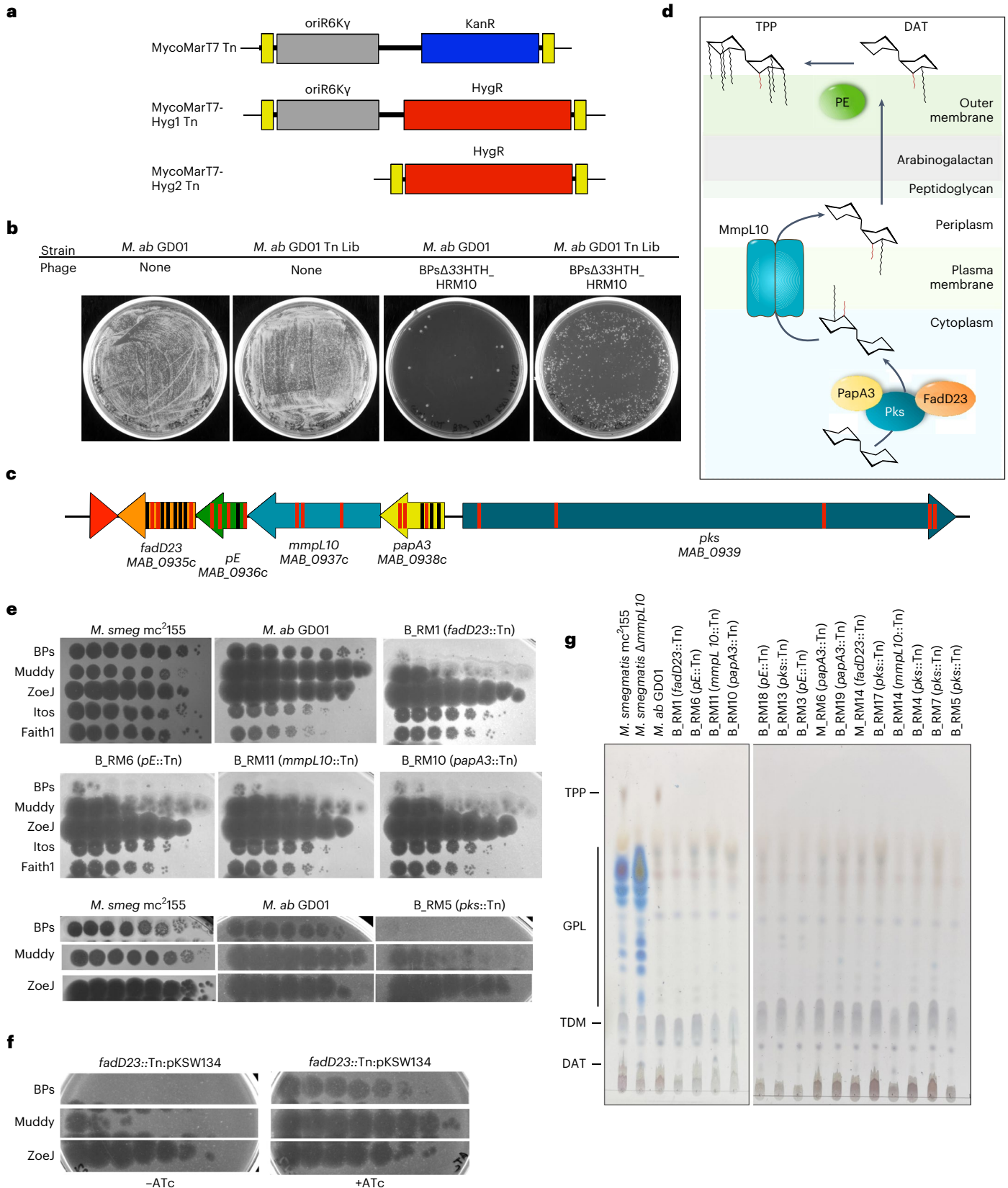
**Fig. 1 | Identification of phage-resistant transposon insertion mutants of *M. abscessus* GD01.** **a**, Construction of MycoMarT7-Hyg1 and MycoMarT7-Hyg2. Transposon delivery phage phiMycoMarT7 delivers a transposon containing *Escherichia coli* ori6Kγ (grey) and a kanamycin resistance cassette (blue), flanked by inverted repeats (yellow boxes). CRISPY-BRED<sup>31</sup> was used to create phiMycoMarT7-Hyg1 and phiMycoMarT7-Hyg2, which deliver transposons containing ori6Kγ (grey box) and a hygromycin resistance cassette (red box), or only a hygromycin resistance cassette. **b**, *M. abscessus* GD01 or a transposon library of *M. abscessus* strain GD01 (*M. ab* GD01 Tn Lib) was plated on solid media or solid media seeded with phage BPs\_Δ33HTH\_HRM10. **c**, Locations of transposon insertions in the TPP locus in phage-resistant mutants. Red and black bars show the locations of insertions in strains isolated as resistant to BPsΔ33HTH\_HRM10 and Muddy, respectively. **d**, Proposed roles of Pks, PapA3, FadD23, MmpL10 and PE in the synthesis and transport of TPPs and DAT. **e**, Tenfold serial dilutions of phages were spotted onto solid media with *M. smegmatis* mc<sup>2</sup>155, *M. abscessus* GD01 or representative *M. abscessus* GD01

transposon insertion mutant strains: GD01Tn\_BPs\_HRM10\_RM1 (B\_RM1); GD01Tn\_BPs\_HRM10\_RM6 (B\_RM6); GD01Tn\_BPs\_HRM10\_RM11 (B\_RM11); GD01Tn\_BPs\_HRM10\_RM10 (B\_RM10); GD01Tn\_BPs\_HRM10\_RM5 (B\_RM5). The locations of Tn insertions are indicated in parentheses. Phages used are: BPsΔ33HTH\_HRM10 (‘BPs’), Muddy, ZojΔ43–45 (‘Zoj’), Itos and Faith1Δ38–40 (‘Faith1’). Plaque assays were performed at least twice with similar results. **f**, Tenfold serial dilutions of phages were spotted onto solid media with strain GD01fadD23::Tn (GD01Tn\_BPs\_HRM10\_RM1) containing plasmid pKSW134 with gene *fadD23* under expression of an ATc-inducible promoter. FadD23 is not expressed in the absence of ATc (left panel) but is induced by ATc (right panel). Plaque assays were performed at least twice with similar results. **g**, Thin-layer chromatography (TLC) analysis of total lipids extracted from *M. abscessus* GD01 and mutants with transposon insertions in the TPP synthesis and transport genes. *M. smegmatis* mc<sup>2</sup>155 and a Δ*mmpL10* mutant strain of *M. smegmatis* are also included as controls.

that we tested remain sensitive to ZoeJ $\Delta$ 43–45, Itos and Faith1 $\Delta$ 38–40 (Fig. 1e and Extended Data Fig. 1).

Analysis of cell wall lipids shows that all of the mutants tested have lost TPPs (Fig. 1g). Interruption of TPP precursor transport (as in an *mmpL10* mutant; Fig. 1d), or loss of PE protein needed for the

final step of TPP synthesis (Fig. 1d) can result in accumulation of the DAT precursor<sup>24,26</sup>, and our *mmpL10* transposon insertion mutants did accumulate DAT. Our *pE* mutants did not accumulate DAT and the Tn insertions may be polar, interrupting *fadD23* expression and DAT synthesis (Fig. 1c,d,g). No defects in trehalose dimycolate synthesis



were observed, trehalose dimycolate being transported by MmpL3 (ref. 34) (Fig. 1g).

### Phage BPs tail spike mutants are TPP independent

Although BPs $\Delta$ 33HTH\_HRM10 does not efficiently infect *M. abscessus* TPP synthesis mutants, plaques were observed at high phage titres that are candidates for TPP-independent mutants (Fig. 1e). Five individual plaques were purified, shown to have heritable infection of *M. abscessus* TPP mutants and were further characterized. Two were isolated on *M. abscessus* GD01 *fadD23::Tn* (phKSW2 and phKSW3), two on GD01 *pE::Tn* (phKSW4 and phKSW5) and one on GD180\_RM2 (BPs\_REM1; see below); an additional mutant (phKSW1) was isolated on *M. smegmatis*  $\Delta$ MSMEG\_5439 (Extended Data Table 2; see below). These mutants form clear plaques on all TPP synthesis pathway mutants tested (Fig. 2a), and sequencing showed that all have single amino acid substitutions in the predicted BPs tail spike protein, gp22 (Extended Data Table 2). Interestingly, two of these substitutions, gp22 A306V and A604E (present in phKSW3 and phKSW5, respectively), were reported previously as BPs host range mutants able to infect *M. tuberculosis*<sup>19,29</sup>. The gp22 A604E substitution is also present in phage BPs $\Delta$ 33HTH\_HRM<sup>GD03</sup> that infects some other *M. abscessus* strains<sup>4</sup>. Although phKSW4 (and phKSW2; Extended Data Table 2) has a gp22 L462R substitution, BPs\_REM1 has both a gp22 L462R substitution and a G780R substitution. BPs\_REM1 forms somewhat clearer plaques than phKSW4 on the TPP mutants (Fig. 2a), suggesting that G780R has an additive effect towards clear plaque formation.

### TPPs are required for BPs adsorption to *M. abscessus* GD01

Because TPPs are surface exposed and are required for BPs $\Delta$ 33HTH\_HRM10 infection, we tested whether they are required for adsorption (Fig. 2b). Wild-type BPs adsorb relatively poorly to *M. smegmatis*<sup>19</sup> and BPs $\Delta$ 33HTH\_HRM10 adsorption is similarly poor on *M. abscessus* GD01 (Fig. 2b). However, BPs $\Delta$ 33HTH\_HRM10 is clearly defective in adsorption to a GD01 *fadD23::Tn* mutant (Fig. 2b, left panel). Interestingly, the TPP-independent phage phKSW1 (Extended Data Table 2) adsorbs considerably faster to GD01 (as does a BPs gp22 A604E mutant in *M. smegmatis*<sup>19</sup>) than its parent phage (Fig. 2b, middle panel) and shows only a small improvement in adsorption to the GD01 *fadD23::Tn* mutant relative to BPs $\Delta$ 33HTH\_HRM10 infection of GD01 (Fig. 2b). In contrast, Zoej $\Delta$ 43–45 adsorbs similarly to both *M. abscessus* strains (Fig. 2b, right panel).

### Phage Muddy tail spike mutants are also TPP independent

We similarly isolated a resistance escape mutant of Muddy (Muddy\_REM1, Extended Data Table 2) and, together with three Muddy mutants with expanded *M. tuberculosis*<sup>20</sup> host ranges, characterized their infection of TPP pathway mutants (Fig. 2c). Three of the mutants (Muddy\_REM1, Muddy\_HRM<sup>N0157-1</sup> and Muddy\_HRM<sup>N0052-1</sup>) efficiently infect all of the TPP pathway mutants; Muddy\_HRM<sup>N0157-2</sup> forms very turbid plaques on all of the mutants, similar to wild-type Muddy (Fig. 2c). Sequencing showed that Muddy\_REM1 contains a single base substitution in the tail spike gene 24 conferring an E680K substitution (Extended Data Table 2), the same substitution as in Muddy\_HRM<sup>N0052-1</sup>; Muddy\_HRM<sup>N0157-1</sup> and Muddy\_HRM<sup>N0157-2</sup> have G487W and T608A substitutions in gp24, respectively<sup>20</sup>.

### Loss of TPPs in spontaneous *M. abscessus* resistant mutants

We previously reported *M. abscessus* mutants spontaneously resistant to BPs derivatives<sup>9</sup>. Two of the strains (GD17\_RM1 and GD22\_RM4, Extended Data Table 3) have mutations in *pks* and are at least partially resistant to BPs $\Delta$ 33HTH\_HRM10 (ref. 9). We have similarly isolated three additional spontaneous mutants resistant to BPs $\Delta$ 33HTH\_HRM10, two of which (GD38\_RM2 and GD59\_RM1) have mutations in *pks*; the third (GD180\_RM2) has a nonsense mutation in *mmpL10* (Extended Data Table 3). BPs $\Delta$ 33HTH\_HRM10 does not form plaques on mutants GD38\_RM2, GD17\_RM1 or GD59\_RM1 and forms very small plaques at a reduced efficiency of plaquing on GD22\_RM4 (Fig. 3a). Thus, point mutations in *M. abscessus* TPP synthesis genes can give rise to BPs resistance, although these have not been observed clinically<sup>5</sup>. These mutants are infected well by other phages we tested that infect the parent strain (Fig. 3a).

The *M. abscessus* Pks protein (MAB\_0939) is a 3,697-residue multi-domain protein (Fig. 3b). Two of the spontaneously resistant mutants have frameshift mutations close to the midpoint of the gene (at codons 2,115 and 2,389, Extended Data Table 3 and Fig. 3b) and two others have amino acid substitutions in the N-terminal ketosynthase (KS) domain (Extended Data Table 3 and Fig. 3b). We note that the two frameshift mutations are in the second acyltransferase (AT) domain and leave the upstream domains intact (Fig. 3b).

### Some phage-insensitive clinical isolates lack TPPs

*M. abscessus* clinical isolates vary greatly in their sensitivity to BPs $\Delta$ 33HTH\_HRM10 and Muddy<sup>9</sup>. There are probably numerous determining factors, but these could include loss of TPPs. Analysis of the TPP synthesis proteins (Pks, PE, PapA3, MmpL10 and FadD23) of 143 sequenced clinical isolates and reference strain ATCC19977 identified 37 distinct genotypes that generally correlate with global nucleotide similarity (Fig. 3c); however, no evident correlation between these variations and sensitivity to BPs $\Delta$ 33HTH\_HRM10 and/or Muddy was observed (Fig. 3c). Most of the variations observed reflect amino acid substitutions, although two strains (GD262 and GD273) have identical large deletions in *pks* (3,645 bp) and two others (GD155 and GD286) have translocations resulting in 30.2 kbp insertions in *pks* (Fig. 3d). Both GD273 and GD286 have phage infection profiles consistent with TPP loss, and the TPP-independent mutant Muddy\_HRM<sup>N0052-1</sup> overcomes the defect (Fig. 3e). GD262, GD273 and GD286 are not susceptible to BPs $\Delta$ 33HTH\_HRM10 or the TPP-independent mutant BPs\_REM1 (Fig. 3e), and these strains probably carry additional phage defence mechanisms targeting BPs and its derivatives. GD155 has a smooth colony morphology (Fig. 3c) and is not susceptible to any of the phages tested here.

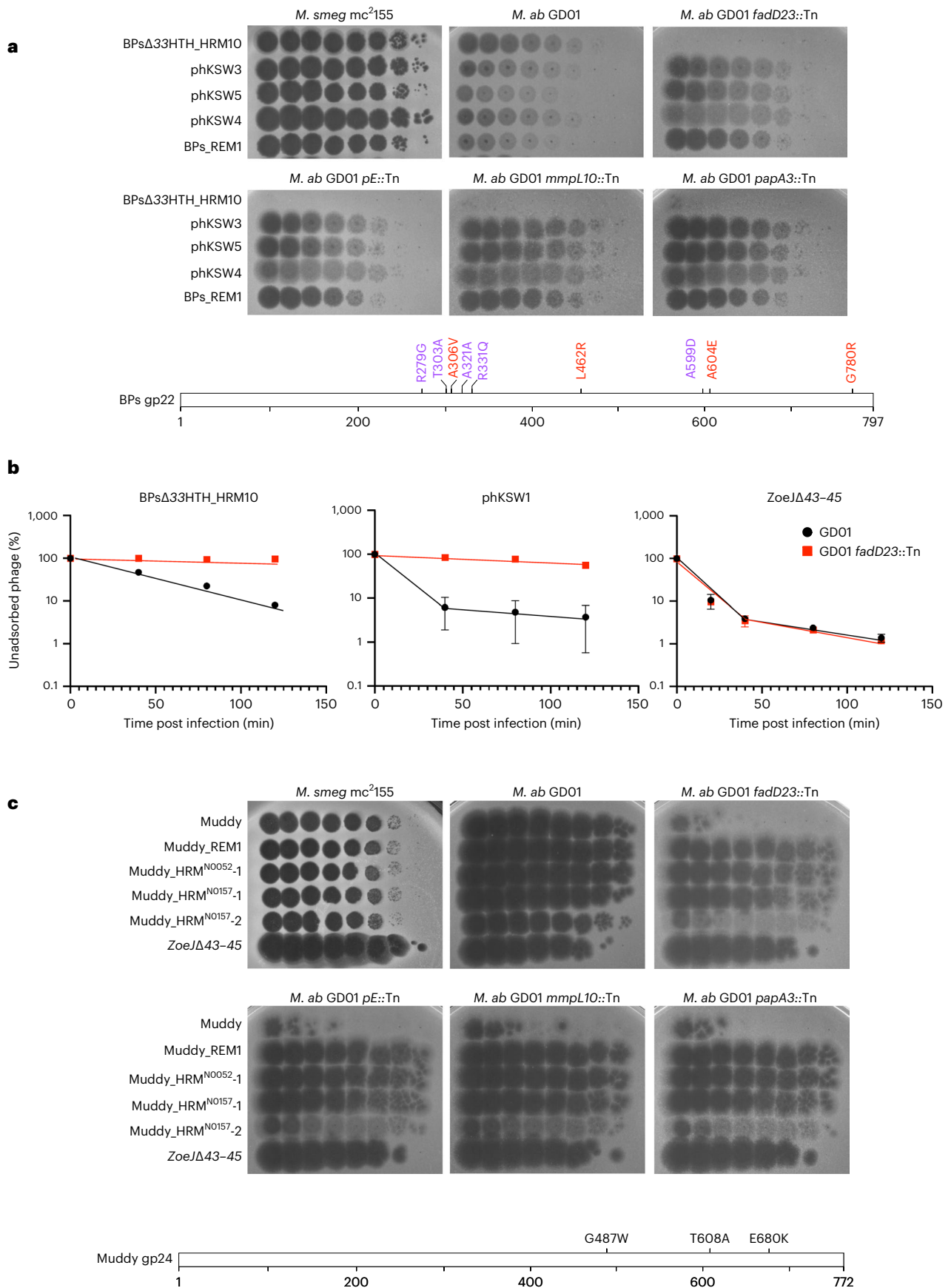
### Complementation restores TPP synthesis and phage infection

Mutants GD22\_RM4 and GD180\_RM2, which are defective in *pks* and *mmpL10*, respectively (Fig. 4a), can both be complemented to fully restore BPs $\Delta$ 33HTH\_HRM10 and Muddy infection (Fig. 4b). Both mutants lack cell wall TPPs and TPPs are at least partially restored by complementation (Fig. 4c). Furthermore, a derivative of BPs expressing mCherry<sup>35</sup>, which behaves similarly to BPs $\Delta$ 33HTH\_HRM10 in plaque assays (Fig. 4b) and liquid infections (Fig. 4d), gives fluorescence from parent strains but not from GD22\_RM4 and GD180\_RM2 (Fig. 4e,f and

### Fig. 2 | Mutants of BPs $\Delta$ 33HTH\_HRM10 and Muddy overcome TPP loss.

**a**, Tenfold serial dilutions of BPs $\Delta$ 33HTH\_HRM10 and gp22 mutants (as indicated on the left; see Extended Data Table 2) were spotted onto solid media with *M. smegmatis* mc<sup>2</sup>155, *M. abscessus* GD01 or *M. abscessus* GD01 transposon insertion mutant strains. Plaque assays were performed at least twice with similar results. The locations of amino acid substitutions in BPs $\Delta$ 33HTH\_HRM10 gp22 conferring the ability to infect TPP-deficient strains (red) or previously found to broaden host range to include *M. tuberculosis* (purple) (bottom panel) are indicated. The A306V and A604E substitutions were identified with both assays. **b**, Adsorption of phages BPs $\Delta$ 33HTH\_HRM10, phKSW1 and Zoej $\Delta$ 43–45 to *M. abscessus*

strains GD01 and GD01 *fadD23::Tn* (GD01Tn\_BPs\_HRM10\_RM1) as indicated by the percentage of unadsorbed phages remaining in infection supernatants at different times after infection. Assays were performed in duplicate twice and data presented are mean  $\pm$  s.d. **c**, Tenfold serial dilutions of Muddy and Muddy gp24 mutants (as indicated on the left) were spotted onto solid media with *M. smegmatis* mc<sup>2</sup>155, *M. abscessus* GD01 or *M. abscessus* GD01 transposon insertion mutant strains. Plaque assays were performed at least twice with similar results. The locations of amino acid substitutions in Muddy gp24 that confer the ability to infect TPP-deficient strains (bottom panel) are indicated.



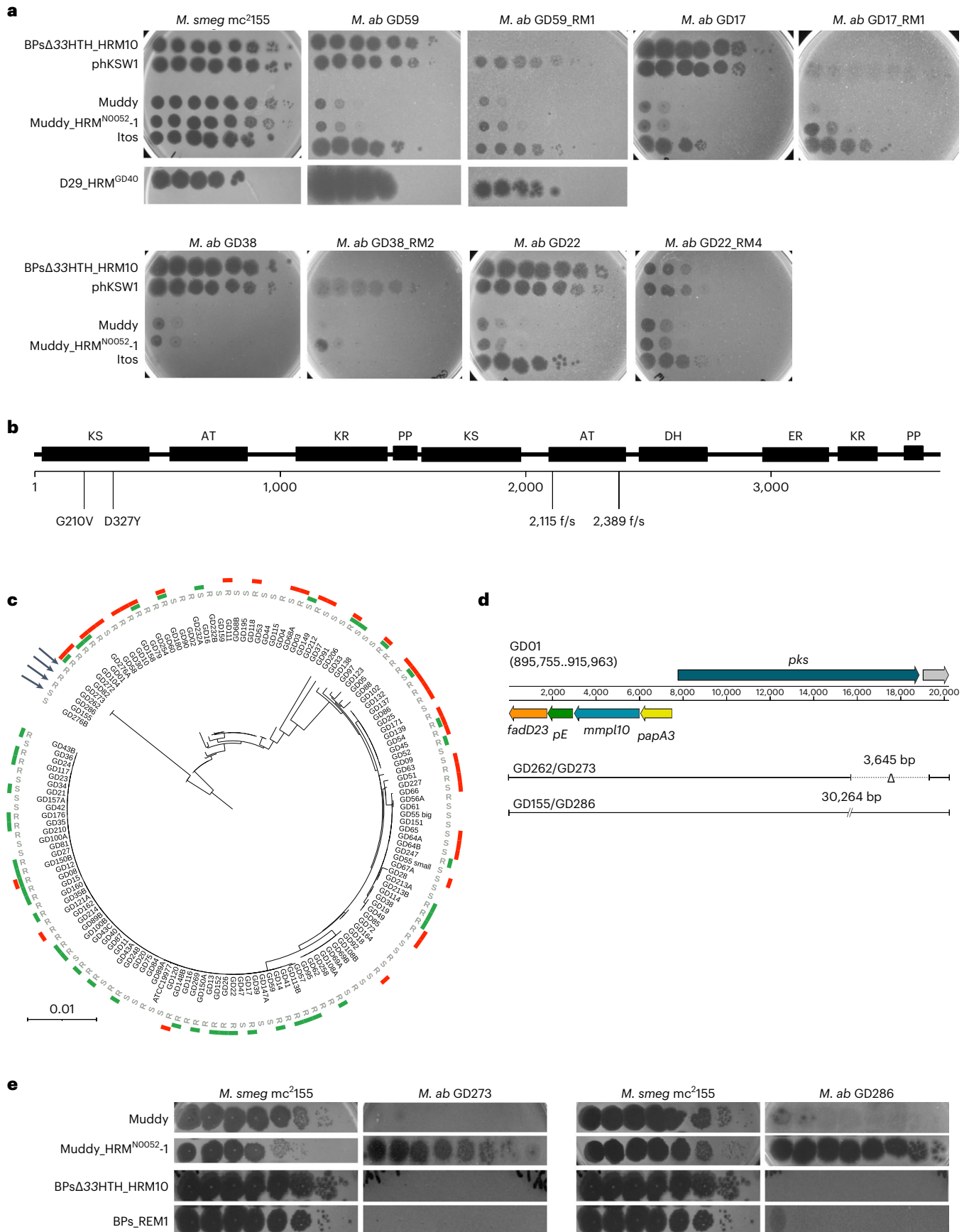


**Fig. 3 | Phage infection profiles of *M. abscessus* phage-resistant mutants.**

**a**, Tenfold serial dilutions of phage lysates (as indicated on the left) were spotted onto solid media with *M. smegmatis* mc<sup>2</sup>155, the parent *M. abscessus* strains or spontaneously isolated phage-resistant mutant (RM) derivatives. Plaque assays were performed at least twice with similar results. **b**, A schematic representation of *M. abscessus* Pks showing the location of predicted functional domains and the amino acid changes in spontaneous phage-resistant mutants below. Domain abbreviations are: AT, acyltransferase; KS, ketosynthase, KR, ketoreductase; DH, dehydratase; ER, enoylreductase; PP, phosphopantetheinylate acyl carrier protein. Domains were identified using the PKS analysis web site at <http://nrps.igs.umd.edu/> (ref. 53). **c**, Amino acid sequences from the five TPP synthesis

pathway genes in 143 *M. abscessus* clinical isolates (and *M. abscessus* ATCC19977) were concatenated and used to construct a phylogenetic tree. Strain morphotypes are labelled as either rough (R) or smooth (S). Susceptibilities to phages BPsΔ33HTH\_HRM10 and Muddy are represented in green and red, respectively<sup>9</sup>. Arrows indicate strains in **d** and **e**. **d**, Position of large deletions (GD262 and GD273) or insertions (GD155 and GD286) in the *pks* gene with respect to the GDO1 TPP locus. **e**, Tenfold serial dilutions of phage lysates (as indicated on the left) were spotted onto solid media with either *M. smegmatis* mc<sup>2</sup>155 or *M. abscessus* strains GD273 and GD286. Plaque assays were performed at least twice with similar results.

Extended Data Fig. 2). Complementation fully restores liquid infection of GD180\_RM2 and partially restores infection of GD22\_RM4 (Fig. 4d), as well as fluorescence with the reporter phage (Fig. 4e,f). These data are consistent with an early defect in phage infection in these mutants, consistent with loss of adsorption to the cell surface. We note that disruption of TPP synthesis does not interfere with Ziehl-Neelsen staining of the bacteria or alter antibiotic sensitivities (Extended Data Fig. 3).

***M. smegmatis* TPP mutants are resistant to BPs and Muddy**

*M. smegmatis* is genetically tractable and susceptible to a large number of diverse phages, and using TPP mutants in *pks* (*MSMEG\_0408*), *papA3* (*MSMEG\_0409*), *mmpL10* (*MSMEG\_0410*), *fadD23* (*MSMEG\_0411*) and *pE* (*MSMEG\_0412*)<sup>24,36</sup>, we showed that these have similar, albeit somewhat milder, phenotypes to *M. abscessus* TPP mutants (Fig. 5a). As expected, Δ*pks*, Δ*mmpL10* and Δ*pE* mutants failed to produce TPPs, while complementation restores the presence of TPPs (Fig. 5b). The relatively efficient infection of the Δ*fadD23* mutant is consistent with incomplete TPP loss, possibly due to an unidentified fatty acyl-AMP ligase partially overcoming the defect<sup>24</sup>. Muddy similarly forms very turbid plaques on the Δ*pks* and Δ*papA3* mutants, but only mildly so on the Δ*fadD23* mutant (Fig. 5a). Interestingly, the TPP-independent BPs and Muddy mutants infect *M. smegmatis* TPP mutants normally (Fig. 5a). Complementation of the Δ*papA3*, Δ*pks*, Δ*mmpL10* and Δ*pE* mutants restores normal infection by both Muddy and BPsΔ33HTH\_HRM10 (Extended Data Fig. 4).

BPsΔ33HTH\_HRM10 and its mCherry derivatives are both defective in liquid infection of the Δ*pks*, Δ*mmpL10* and Δ*pE* *M. smegmatis* mutants, and efficient infection and lysis are restored by complementation (Extended Data Fig. 4a,e). The mCherry reporter phage shows fluorescence in wild-type *M. smegmatis* but loss of fluorescence in infection of all three mutants, with restoration of infection in the complemented strains (Extended Data Fig. 4b,c). In addition, the mCherry fluorophage behaves similarly to its parent in plaque assays on *M. smegmatis* mutant and complemented strains (Extended Data Fig. 4e). Both BPsΔ33HTH\_HRM10 and the TPP-independent phKSW1 are defective in adsorption of a Δ*pks* mutant relative to wild-type *M. smegmatis* (Fig. 5c and Extended Data Fig. 5), similar to *M. abscessus* (Fig. 2b).

Testing a broader phage panel showed that most are not dependent on TPPs, except for ShedlockHolmes, MsGreen and Papyrus in Clusters/Subclusters K3, L3 and R, respectively, which show some TPP dependence (Fig. 5d). MsGreen and ShedlockHolmes have tail genes

related to Muddy gene 24, although we note that Zoj also does and yet is not TPP dependent. However, such variation is not unexpected, as the escape mutant observations show that only a single amino acid substitution is sufficient to confer TPP independence (Figs. 2a,c and 5a).

**TPP-independent phages reveal host resistance mechanisms**

The TPP-independent phage mutants infect *M. abscessus* efficiently and we therefore repeated the selection for Tn insertion mutants to explore whether there are other surface molecules required for infection. Interestingly, such mutants arise from the same library at a 100-fold lower abundance than BPsΔ33HTH\_HRM10 and Muddy resistant mutants (Fig. 6a and Extended Data Table 1). All but one of the phKSW1 resistant mutants analysed are similarly resistant to BPsΔ33HTH\_HRM10, BPs\_REM1 and phKSW1 but remain sensitive to Muddy and Muddy\_REM1 (Fig. 6b); one (GDO1Tn\_phKSW1\_RM10) is resistant to phKSW1 but is sensitive to BPs\_REM1 and is resistant to Muddy but not Muddy\_REM1 (Fig. 6b). One of the two Muddy\_REM1 resistant mutants is only partially resistant to Muddy and Muddy\_REM1, but both are fully sensitive to all of the BPs derivatives (Fig. 6b).

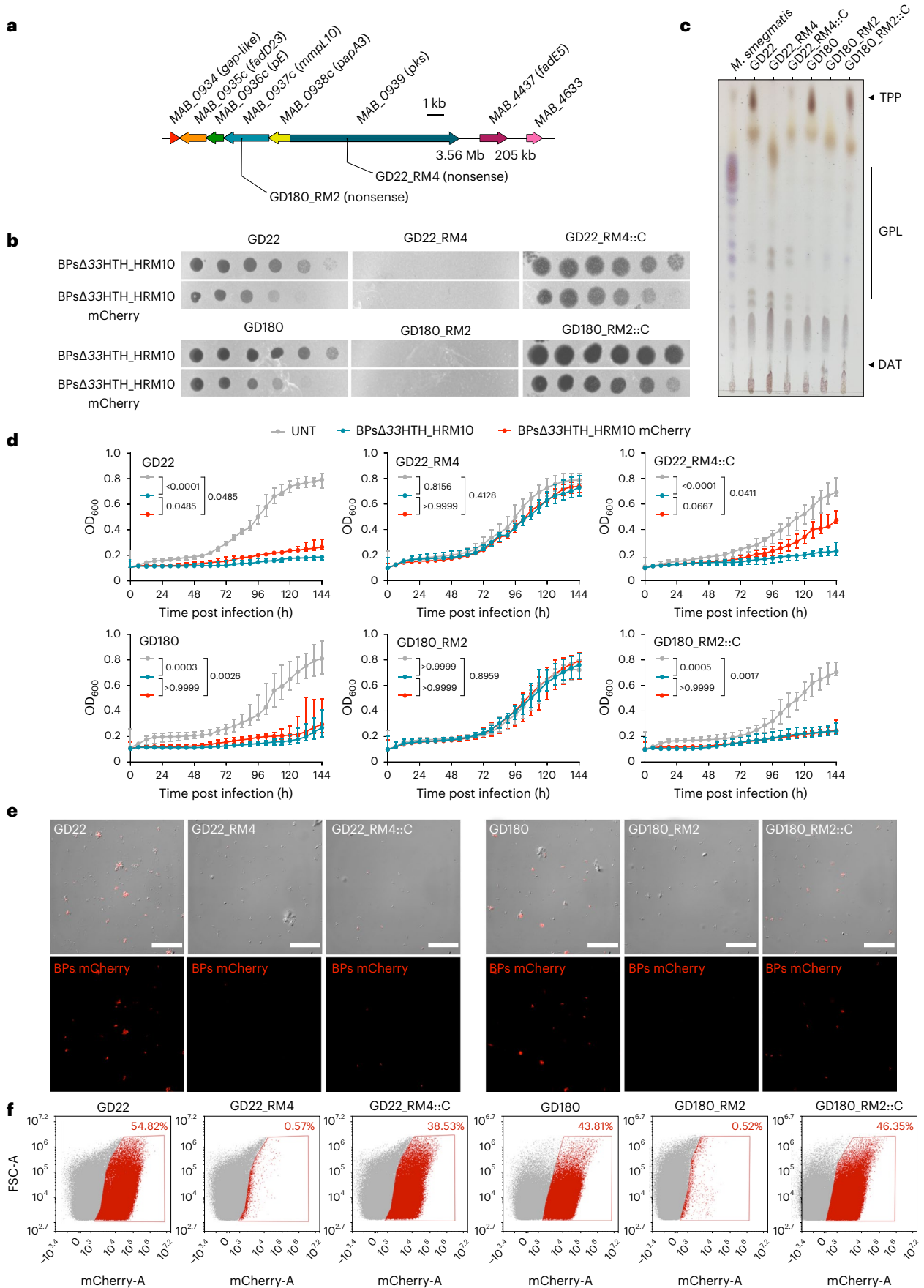
Characterization of these mutants shows that they are unlikely to be defective in surface recognition by the phages. Two Muddy\_REM1 resistant strains have Tn insertions in transcription genes *greA* and *rpoC* (Extended Data Table 1), and one phKSW1 resistant mutant maps in *recB* (*MAB\_0399c*; Extended Data Table 1); these are unlikely to be directly involved in phage binding. Four of the phKSW1 resistant mutants (RM2, RM5, RM7 and RM8), representing at least three independent insertions (Fig. 6 and Extended Data Table 1), have transposons at GDO1 coordinate 1,169,901 in a region absent from ATCC19977 and many other *M. abscessus* strains and within a candidate 'phage-inducible chromosomal island' (PICl) (Fig. 6c and Extended Data Table 1). The insertions are upstream of GDO1 gene *EXM25\_05825* encoding a protein with a DUF4145 domain, which is implicated in a variety of viral defence systems and is often fused with restriction endonucleases and abortive infection systems<sup>37–39</sup> (Fig. 6c). It is plausible that the BPs resistant phenotype results from overexpression of this gene.

Analysis of the cell wall lipids shows that all of the mutants retain TPPs, except for GDO1Tn\_phKSW1\_RM10 (Fig. 6d), which has a Tn insertion in *papA3* in addition to a secondary insertion in *MAB\_1686* (Extended Data Table 1). Two additional mutants (GDO1Tn\_phKSW1\_RM1 and RM4) have an insertion in the nearby *MAB\_1690* gene and have normal TPPs (Fig. 6d); *MAB\_1686* and *MAB\_1690* are within a large

**Fig. 4 | TPPs are essential for BPsΔ33HTH\_HRM10 to lyse *M. abscessus*.**

**a**, Representation of the *M. abscessus* TPP locus showing mutations affecting the clinical strains studied. **b**, Phages were spotted as tenfold serial dilutions onto clinical strains (GD22 and GD180), spontaneous resistant mutants (RM) and complemented strains (::C). Plates were incubated for 2–3 d at 37 °C before imaging. The assay was repeated at least three times and a representative experiment is shown. **c**, TLC analysis of total lipids extracted from *M. abscessus* clinical strains, resistant mutants and complemented strains. Eluent: CHCl<sub>3</sub>/CH<sub>3</sub>OH (90:10 v/v). Anthrone was sprayed on the plates to visualize the lipid profile, followed by charring. **d**, Liquid growth of the strains with BPsΔ33HTH\_HRM10 or BPsΔ33HTH\_HRM10 mCherry (MOI10) or without phage (untreated; UNT)

monitored every 6 h for 6 d at 37 °C in 7H9/OADC supplemented with 1 mM CaCl<sub>2</sub>. Data are plotted as the median ± interquartile range of three independent experiments done in triplicate. Statistical analysis conducted to compare the differences at 144 h between strains was done with a two-sided Dunn's multiple comparisons test, with *P* values indicated. **e**, Representative fields of *M. abscessus* clinical strains infected with BPsΔ33HTH\_HRM10 mCherry (MOI 10) for 4 h at 37 °C before fixation. Infected bacilli appear in red. These results were obtained at least two times. Scale bars, 30 μm. **f**, Flow cytometry data represented as dot plot show the percentage of bacilli infected with the BPsΔ33HTH\_HRM10 mCherry fluorophage relative to the study population. This assay was conducted at least twice.





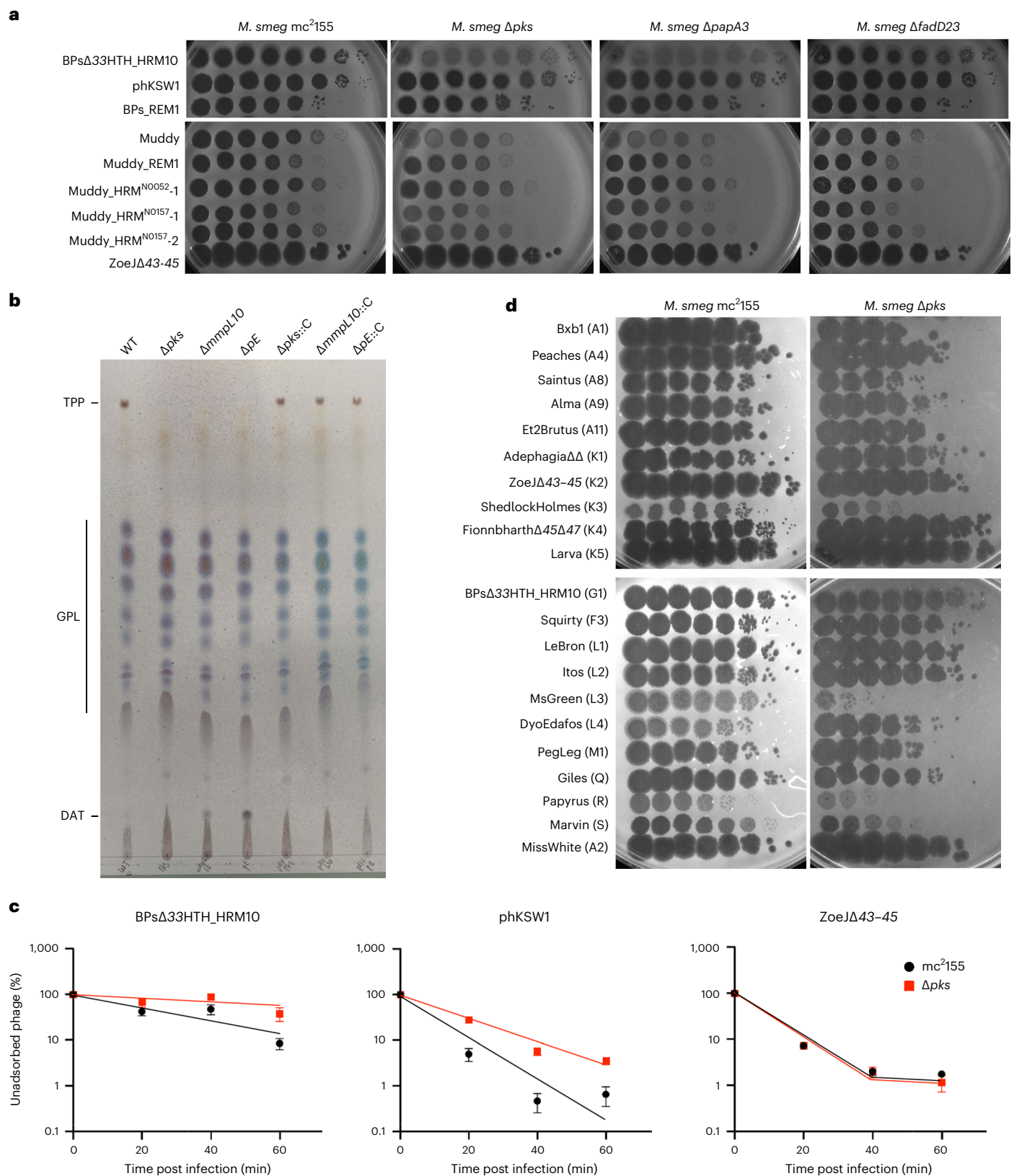


**Fig. 5 | TPPs are also required for infection of *M. smegmatis* by phages BPs and Muddy. a**, Tenfold serial dilutions of phages (as indicated on the left) were spotted onto solid media with *M. smegmatis* mc<sup>2</sup>155, Δ*pks*, Δ*papA3* or Δ*fadD23* as indicated. Plaque assays were performed at least twice with similar results. **b**, TLC analysis of total lipids extracted from wild-type *M. smegmatis*, three TPP-deficient mutants and the corresponding complemented strains. Eluent: CHCl<sub>3</sub>/CH<sub>3</sub>OH (90:10 v/v). TLC was revealed by spraying anthrone on the plate, followed by charring. **c**, Adsorption of phages BPsΔ33HTH\_HRM10, phKSW1 and ZoeJΔ43-45 to *M. smegmatis* strains

mc<sup>2</sup>155 and Δ*pks* as indicated by the percentage of unadsorbed phages remaining in the supernatant at different times after infection. Assays were performed in triplicate at least twice with similar results and a representative experiment is shown. Data are represented as mean ± s.d. Other replicates are shown in Extended Data Fig. 5. **d**, A panel of phages from various genetic clusters were tenfold serially diluted and spotted onto *M. smegmatis* mc<sup>2</sup>155 and Δ*pks*. Phage names are shown with their cluster/subcluster designation in parentheses. Plaque assays were performed twice with similar results.

(22 kbp) operon encoding an Mce4 transport system (Extended Data Table 1). However, this Mce4 system is probably not acting as a receptor as the GD01Tn\_phKSW1\_RM1 mutant does not have an adsorption defect (Fig. 6e). The GD01Tn\_phKSW1\_RM2 mutant also does not have any adsorption defect (Fig. 6e).

## Discussion

Trehalose polyphosphates are among the largest known lipids in mycobacteria and are structurally related to sulfolipids SL-1 and polyacylated trehalose PAT, which, in contrast to TPPs, are found exclusively in *M. tuberculosis*. The roles of TPPs in mycobacterial physiology and/or growth remain unclear, but they are implicated in clumping and cording in *M. abscessus*<sup>25</sup>. Many TPP-defective *M. abscessus* strains have rough morphotypes, typically associated with cording, consistent with the rough colony morphology primarily resulting from GPL loss<sup>23</sup>. Clearly, TPPs are critical for adsorption of several phages, including the therapeutically useful Muddy and BPs<sup>4,5</sup>. The finding that both phages require TPPs is a surprise, as they are genomically distinct, share few genes and were thus considered to be suitable for combination in phage cocktails. Nonetheless, the availability of TPP-independent phage mutants provides substitutes to which resistance to both phages occurs at a much lower frequency, and such mutants do not typically show co-resistance to the two phages. We propose that the TPP-independent phages replace their cognate parent phages in therapeutic cocktails.

A simple explanation for the role of TPPs is that they are specifically recognized and bound to by BPs, Muddy and the other TPP-dependent phages as the only requirement for DNA injection. However, it is then unclear as to how the TPP-independent phages overcome TPP loss, and it seems implausible that they gain the ability to bind to a completely different receptor. A more likely explanation is that TPPs act as co-receptors for Muddy and BPs and facilitate recognition of a different surface molecule; the TPP-independent phage mutants would then simply bypass the need for activation by TPPs. The observation that tail spike mutants such as phKSW1 adsorb substantially better than the parent phage, even to TPP-containing host cells, is consistent with this latter explanation. Furthermore, wild-type BPs does not efficiently infect *M. tuberculosis* H37Rv, but a mutant with the gp22 A604E substitution enables efficient infection<sup>19</sup>, even though *M. tuberculosis* lacks TPPs<sup>40</sup>. Similarly, wild-type Muddy efficiently infects *M. tuberculosis* H37Rv<sup>20</sup> despite its lack of TPPs, and Muddy tail spike substitutions expand its host range to other *M. tuberculosis* strains<sup>20</sup>. These observations not only suggest that TPPs are not the receptors per se for these phages, but that there may be general mechanisms governing receptor access by the phages, together with phage strategies for expanding host cell recognition and infection. Furthermore, if TPPs are not the target of direct phage recognition, the true receptor is likely to be encoded by genes that are essential for mycobacterial viability. Thus, although transposon insertion mutagenesis has been used in other systems for identifying phage receptors<sup>41–44</sup>, this may be of more limited use

in *Mycobacterium*, although as we have shown here, it is useful for mapping a plethora of resistance mechanisms.

Understanding the roles of TPPs in *M. abscessus* is important for therapeutic phage use, and we note that in at least some clinical isolates, the loss of TPPs through gene deletions or translocation leads to loss of infection by BPsΔ33HTH\_HRM10 or Muddy. In the first therapeutic use of mycobacteriophages, BPsΔ33HTH\_HRM10 and Muddy were used in combination with Zoj, and it is of interest that Zoj is not TPP dependent. We also note that resistance to BPs derivatives or Muddy has not been observed in clinical use, even in 11 cases where only a single phage was used<sup>5</sup>. It is plausible that resistance through TPP loss has a trade-off with fitness, although the roles of TPPs in *M. abscessus* pathogenicity and persistence are not known. Strikingly, the use of TPP-independent derivatives of BPs and Muddy not only avoids concerns about resistance via TPP loss, but also negates cross-resistance between the two phages (Fig. 6).

Finally, transposon mutagenesis and selection of mutants resistant to the TPP-independent phages reveal additional mechanisms of phage resistance. Particularly intriguing is the isolation of insertions in a candidate PIC1, with the potential to activate expression of a PIC1 gene implicated in phage defence. These *Mycobacterium* PIC1s and their roles in phage infection profiles deserve further investigation.

## Methods

### Bacterial strains and culture conditions

Bacterial strains (Extended Data Table 4) were grown in Middlebrook 7H9 media (BD Difco) supplemented with 10% oleic acid, albumin, dextrose and catalase (OADC enrichment) (7H9/OADC), or in Middlebrook 7H10/OADC solid media (BD Difco) at 37 °C. Antibiotics were added when required. Transformations of electrocompetent mycobacteria were performed using a Bio-Rad Gene pulser (25 μF, 2,500 V, 800 Ω). For some *M. smegmatis* strains, Tween80 (0.05%) was used in starter cultures but omitted in subcultures used for phage infections. Cultures used in phage infection were supplemented with 1 mM CaCl<sub>2</sub>. When required, *M. abscessus* strains were selected with 1 mg ml<sup>-1</sup> hygromycin (Toku-E, 31282-04-9) or 200 μg ml<sup>-1</sup> streptomycin, and *M. smegmatis* was selected with 50 μg ml<sup>-1</sup> hygromycin. *M. abscessus* strains in the GDxx series are part of the strain collection at the University of Pittsburgh and were kindly provided by numerous colleagues.

### Engineering of MycoMarT7-Hyg2

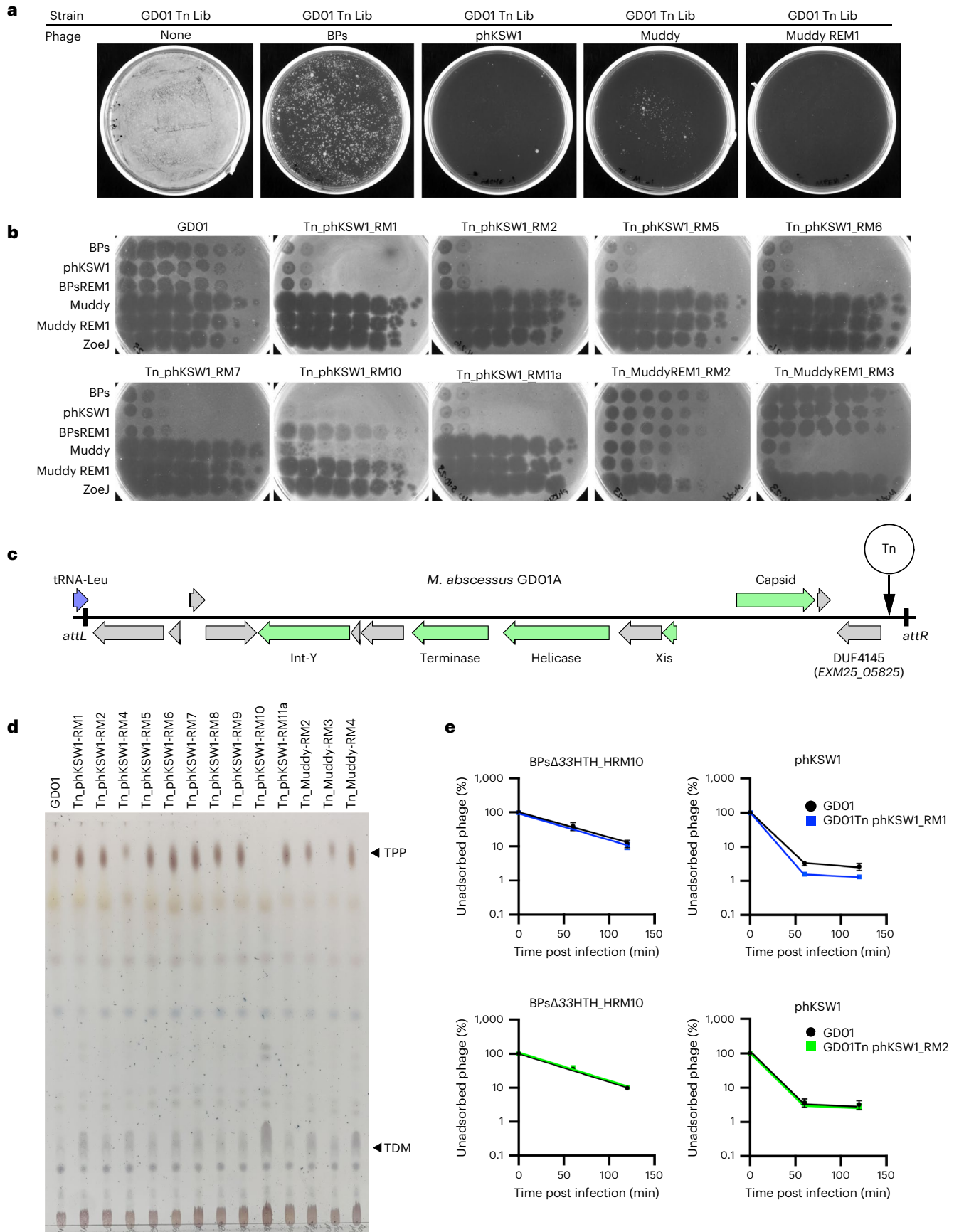
Phage MycoMarT7-Hyg1 and MycoMarT7-Hyg2 were engineered from phage MycoMarT7 using CRISPY-BRED recombineering<sup>31</sup>. Briefly, double-stranded DNA recombineering substrates were designed that contained the desired mutation (a HygR cassette) with flanking sequences to permit the replacement of either KanR (MycoMarT7-Hyg1) or KanR and oriR6K (MycoMarT7-Hyg2). These substrates and genomic (g)DNA from MycoMarT7 were transformed into *M. smegmatis* mc<sup>2</sup>155 recombineering cells that contain the plasmid pJV138 (ref. 31). Transformations were combined with cells containing a CRISPR plasmid

**Fig. 6 | Evidence for additional phage resistance mechanisms.** **a**, Recovery of *M. abscessus* GD01 transposon mutants resistant to phages BPs, phKSW1, Muddy and Muddy\_REM1. A culture of an *M. abscessus* GD01 transposon library (GD01 Tn Lib) containing approximately 10<sup>6</sup> c.f.u. was plated onto phage-seeded plates as indicated. **b**, Phage infection profiles of resistant mutants. Tenfold serial dilutions of phages BPsΔ33HTH\_HRM10 ('BPs'), phKSW1, Muddy, Muddy\_REM1 and ZojΔ43–45 ('Zoj') (as indicated on the left) were spotted onto lawns of *M. abscessus* GD01 or mutants isolated as resistant to TPP-independent phages phKSW1 and Muddy\_REM1. Mutant designations indicate that they are Tn insertions (Tn), the phage used for mutant selection (that is, phKSW1 or Muddy\_REM1) and the mutant number (for example, RM1, RM2 and so on). Where siblings are suspected (Extended Data Table 1), only one representative is shown; suspected siblings showed similar results. **c**, Organization of a putative candidate PIC1 in *M. abscessus* GD01. The satellite region is defined by the *attL*

and *attR* attachment sites resulting from site-specific integration at a tRNA-Leu gene (GD01 coordinates 1158039 to 1170246). It contains several phage-related genes (green arrows) with the putative functions indicated. At the extreme right-hand end of the PIC1, a gene (locus tag EXM25\_05825) carries a DUF4145 domain implicated in phage defence in other systems. Four mutants contain a Tn insertion at the site, indicated by the vertical arrow. **d**, TLC analysis of total lipids extracted from *M. abscessus* GD01 and transposon mutants isolated as resistant to TPP-independent phages. **e**, Adsorption of BPsΔ33HTH\_HRM10 and phKSW1 to GD01Tn\_phKSW1\_RM1 (blue, top panels) and to GD01Tn\_phKSW1\_RM2 (green, bottom panels). Adsorption to GD01 performed in parallel is shown in black. The proportions of phage particles remaining in solution are shown at different times after infection. Assays were performed in duplicate twice and data presented are mean ± s.d.

(a derivative of pIRL53) selecting against the parent MycoMarT7 and plated on solid media; this enriches for mutants containing the allelic replacement that form plaques on the plate. Resulting plaques were

screened for the presence of the Hyg-marked transposon by PCR, and positive plaques were plaque purified, whole-genome sequenced and confirmed to have retained temperature sensitivity.



## Construction of the *M. abscessus* GD01 transposon insertion library and phage challenge

The transposon mutagenesis library was largely prepared as previously described<sup>32</sup>. Briefly, 50 ml of *M. abscessus* GD01 was grown to an OD<sub>600</sub> of 0.2. The cells were pelleted and resuspended in 1 ml of phage buffer (10 mM Tris HCl (pH 7.5), 10 mM MgSO<sub>4</sub>, 68.5 mM NaCl, 1 mM CaCl<sub>2</sub>), pre-warmed to 37 °C and infected with 800 µl MycoMarT7-Hyg2 (5 × 10<sup>10</sup> plaque-forming units (p.f.u.) ml<sup>-1</sup>). The cells and MycoMarT7-Hyg2 were incubated at 37 °C for 7.5 h. Cells were pelleted and resuspended in 8 ml PBS + 0.05% Tween80, and the resuspension was combined with 8 ml 40% glycerol for freezing at -80 °C. The transduction frequency was determined by measuring hygromycin-resistant colonies per ml and 120,000 transductants were plated onto large square plates containing solid 7H10/OADC media with 0.1% Tween80 and 1 mg ml<sup>-1</sup> hygromycin. Plates were incubated at 37 °C for 9 d. To collect the library, cells were scraped off the solid media, resuspended in 7H9/OADC combined with 40% glycerol, aliquoted and frozen at -80 °C.

To identify GD01 insertion mutants that were resistant to phage infection, ~20 µl of GD01 Tn library was thawed and grown overnight to an OD<sub>600</sub> of 0.175. Dilutions of this culture (approximately 10<sup>4</sup>, 10<sup>5</sup> and 10<sup>6</sup> cells) were spread onto 7H10/OADC solid media plates seeded with or without 10<sup>8</sup> p.f.u. of phages BPsΔ33HTH\_HRM10, Muddy, pHKSW1 or Muddy\_REM1. Plates were incubated at 37 °C for 7 d. Colonies able to grow on phage-seeded plates were subjected to PCR to identify a transposon insertion site (see below) and struck out two times to remove any remaining phage. After streaking, single colonies were grown in liquid media and used for phage susceptibility testing by standard plaque assay.

## Identification of transposon insertion sites

Transposon insertion sites were identified by PCR using a primer that annealed to the transposon in the hygromycin resistance gene (Tn\_Hyg\_Fwd\_2: 5'-CTTCACCTTCCTGCACGACT-3') and a primer with a degenerate 3' end, or if that did not yield an amplicon, nested PCR with primers Tn\_Hyg\_Fwd\_2 and Primer 557 (5'-GGCCAGCGACTAACGACANNNNNNNGTT-3') followed by PCR with primers Primer 414 (5'-GGCCAGCGACTAACGAGAC-3') and Tn\_Hyg\_Fwd\_1 (5'-TTCGAGGTGTTTCGAGGAGAC-3'). Amplicons were gel extracted, Sanger sequenced from the transposon and the result aligned to the GD01 sequence to identify the transposon insertion site. For most strains (and at least one strain per interrupted gene), the transposon insertion site was confirmed by designing primers that flanked the site identified by the initial PCR and confirming that this region had increased in size by 1,259 bp compared with strain GD01. For five strains resistant to pHKSW1 (GD01Tn\_pHKSW1\_RM1, 2, 4, 6 and 10), the entire genomes were also sequenced as previously described<sup>9</sup> (and see below) to confirm the location of inserted transposons. Reads were assembled into contigs and the location of the transposon sequence was identified. To confirm the total number of transposon insertions, reads at the transposon/chromosome boundaries were closely inspected to determine the number of branches, and the coverage of the transposon contig compared to the rest of the genome was determined. In the cases of RM1, 2 and 4, the transposon contig had approximately the same coverage as the rest of the genome and showed only one type of transposon/chromosome hybrid read at each end. In the cases of RM6 and 10, the transposon contig had approximately twice the coverage of the rest of the genome, and at each end, there were two types of transposon/chromosome hybrid read.

## Phages and screening of phage susceptibility

Phages used in this study were obtained from the University of Pittsburgh and *M. smegmatis* mc<sup>2</sup>155 was used to propagate them. Phage ZoeJΔ43–45 is a derivative of the previously described ZoeJΔ45 (ref. 28) and contains a deletion of genes 43 (integrase), 44 and 45 (repressor), corresponding to ZoeJ coordinates 33972–36489.

It also contains the following single nucleotide polymorphisms different from ZoeJ: G3204T, A10165G, A10713G, C15262T. Phage susceptibility profiles were assessed using standard plaque assays. Top agar bacterial lawns were made by combining Middlebrook top agar (Middlebrook 7H9, 1 mM CaCl<sub>2</sub>, 0.35% BactoAgar) with 300–500 µl cell culture. After top agar had solidified, phages were tenfold serially diluted and spotted onto the top agar bacterial lawns and incubated for 24–48 h (*M. smegmatis*) or 5–7 d (*M. abscessus*) until bacterial lawns were confluent.

## Plasmid construction

To create plasmid pKSW131, *fadD23*, *pE*, *mmpL10* and *papA3* and the flanking intergenic sequence was amplified using Q5 HiFi2× master mix (New England Biolabs) from gDNA isolated from *M. abscessus* GD01. The amplicon was purified and cloned into EcoRI-digested vector pLA155 using the NEBuilder HiFi DNA Assembly master mix (New England Biolabs) and transformed into *E. coli* strain DH5a; plasmids and primers are shown in Extended Data Table 5. The culture that yielded a successfully constructed plasmid was grown at 30 °C rather than 37 °C, although it is unknown whether this contributed to successful plasmid maintenance in the culture. To create plasmid pKSW134, the open reading frame of *fadD23* was amplified from GD01 gDNA and cloned into PmlI-digested anhydrotetracycline (ATc)-inducible vector pCCK39 (ref. 45) using the NEBuilder HiFi DNA Assembly master mix. The entire plasmids were sequenced using Plasmidsaurus (<https://www.plasmidsaurus.com/>).

pMVpks\_ *mWasabi* and pMVmmpL10\_ *mWasabi* were constructed on the basis of pMVpks and pMVmmpL10 by in-fusion cloning. The *mWasabi* sequence under the control of the constitutive *Pleft\** promoter<sup>46</sup> was amplified by PCR using a Q5 high-fidelity DNA polymerase (New England Biolabs). Plasmids were linearized with KpnI-HF (New England Biolabs). Agarose gels were used to purify linear fragments, then circularized using In-Fusion SNAP Assembly master mix (Takara) according to the manufacturer's instructions. Stellar competent cells (Takara) were used for transformation. Plasmids generated were verified by sequencing (Eurofins Scientific).

## Isolation and whole-genome sequencing of phage-resistant mycobacteria mutants

Two of these phage-resistant mutants (GD17\_RM1 and GD22\_RM4) were described previously<sup>9</sup>; the others were isolated in the same manner. Briefly, 10<sup>8</sup> colony-forming units (c.f.u.) of *M. abscessus* were incubated with 10<sup>9</sup> p.f.u. of phage. Infections were plated on solid media at 2 and 5 d post infection, and survivors were purified, tested for phage resistance and sequenced. The mutants were sequenced as described previously<sup>9</sup>. Briefly, 3 ml of culture was pelleted and resuspended in 600 µl nuclei lysis solution (Promega). Cells were added to lysing matrix B tubes (MP Biomedicals) and milled four times using a Bead-Bug6 microtube homogenizer (BenchMark). RNase A (2 µl, Thermo Scientific) was added and the solution was incubated at 37 °C for 10 min. Phenol-chloroform-isoamyl alcohol was added to the lysed cells and the aqueous phase was removed after centrifugation. DNA was precipitated using isopropanol and 3 M sodium acetate, and washed two times with 75% ethanol before resuspension. Libraries were prepared with the NEBNext Ultra II FS Library Prep kit (New England Biolabs) and sequenced on an Illumina MiSeq. The resulting reads were aligned to the parent strain genome using Consed<sup>47</sup>. A custom programme (AceUtil) was used to identify differences between the mutant reads and the parent genome, and all mutations were confirmed by close inspection of the reads<sup>48</sup>.

## Isolation of BPsΔ33HTH\_HRM10 mutants

Clear plaques were observed within high-titre spots for phage BPsΔ33HTH\_HRM10 on strains GD01Tn\_BPs\_HRM10\_RM6, GD01Tn\_BPs\_HRM10\_RM11 and GD180\_RM2. These plaques were picked and plated on the resistant strain two additional times to purify. A purified

plaque was then used to produce a high-titre phage lysate on *M. smegmatis* mc<sup>2</sup>155 and subsequently subjected to gene 22 PCR sequencing or whole-genome sequencing.

### Total lipids extraction of mycobacteria and TLC analysis

Bacteria were grown in LB medium (Lennox, X964.3) at 37 °C without agitation and pelleted by centrifugation (3,000 g, 10 min, room temperature). Lipids were extracted from bacterial pellets treated successively with CHCl<sub>3</sub>/CH<sub>3</sub>OH (1:2) (Carlo Erba, 67-66-3; Honeywell, 67-56-1) and CHCl<sub>3</sub>/CH<sub>3</sub>OH (2:1), washed with water and dried. Lipids were resuspended in CHCl<sub>3</sub> before spotting on TLC. For TLC analysis, silica gel G60 plates (10 × 20 cm, Macherey-Nagel) were used to spot samples and lipids were separated with CHCl<sub>3</sub>/CH<sub>3</sub>OH (90:10 v/v). Lipid profiles were shown by spraying the plates with a 0.2% anthrone (Sigma, 90-44-8) solution (w/v) in concentrated H<sub>2</sub>SO<sub>4</sub> (Honeywell, 7664-93-9) and charring.

### Adsorption assays

*M. smegmatis* strains were grown to an OD<sub>600</sub> of 0.5–0.8, then concentrated approximately tenfold to 1.75 × 10<sup>9</sup> ml<sup>-1</sup> in 7H9/10% albumin dextrose complex (ADC)/1 mM CaCl<sub>2</sub>. One millilitre of cells (*M. smegmatis* mc<sup>2</sup>155 or mc<sup>2</sup>155 Δ*pks*) was infected in triplicate in a 12-well plate at a multiplicity of infection (MOI) of 0.001. Cells were incubated at 37 °C with agitation. At each timepoint, 50 μl of liquid was removed and pelleted, and the supernatant that contained unbound phage was titred on *M. smegmatis*. For *M. abscessus* GD01 and *M. abscessus* GD01 *fadD23::Tn*, the same protocol was followed but the strains were grown to an OD<sub>600</sub> of 0.15–0.25 and cells were concentrated approximately tenfold to 6.3 × 10<sup>8</sup> ml<sup>-1</sup> in 7H9/10% OADC/1 mM CaCl<sub>2</sub>.

### Growth curves of mycobacteria incubated with phages

Bacterial growth assays were performed in 96-well plates (Falcon), each well containing 100 μl of bacterial culture and 100 μl of phage lysates or medium as control. Exponential phase cultures of mycobacteria were used and set at 3 × 10<sup>7</sup> c.f.u. ml<sup>-1</sup> in Middlebrook 7H9/OADC supplemented with 1 mM CaCl<sub>2</sub>. Phages were incubated at an MOI of 10 and diluted in 7H9/OADC supplemented with 1 mM CaCl<sub>2</sub>. Measurements were taken every 3 h for *M. smegmatis* strains and every 6 h for *M. abscessus* strains using a spectrophotometer (Tecan, infinite 200 PRO) until stationary phase was reached (2 d for *M. smegmatis* strains and 6 d for *M. abscessus* strains). Plates were incubated at 37 °C without agitation.

### Microscopy and flow cytometry sample preparation

Mycobacteria were subcultured in 7H9/OADC with agitation to obtain exponential phase cultures. Bacteria were concentrated to obtain a sample containing 1.2 × 10<sup>7</sup> c.f.u. (for microscopy) or 6 × 10<sup>6</sup> c.f.u. (for flow cytometry) and then incubated with either medium or phage BPsΔ33HTH\_HRM10 (MOI10) as controls or phage BPsΔ33HTH\_HRM10 mCherry (MOI10). The infections were performed for 2 h and 4 h for *M. smegmatis* and *M. abscessus* strains, respectively, at 37 °C without agitation. After infection, samples were fixed with 4% paraformaldehyde (Electron Microscopy Sciences, EM-15714) for 20 min at room temperature. Samples were then diluted as necessary, depending on the experiment, with 7H9/OADC supplemented with 0.025% tyloxapol and sonicated to disrupt bacterial aggregates. For microscopy, samples were then mounted between coverslips and slides with Immu-Mount (Eprelia). Samples were kept at 4 °C in the dark until analysis.

### Microscopy

Differential interference contrast and epifluorescence images were acquired on a ZEISS Axio Imager Z1 upright microscope. A ×63 Plan Achromat 1.4 NA oil objective and a ×100 Plan Achromat 1.4 NA oil objective were respectively used for *M. smegmatis* and *M. abscessus* strains. mCherry was excited with an Intensilight fibre lamp with Texas

Red (Ex: 560/40, dic. 585, Em: 630/75) filter cube. Images were acquired with an sCMOS ZYLA 4.2 MP camera.

### Image analysis

Representative fields without technical artefacts were chosen. Fiji software (version 1.53t) was used to adjust intensity, brightness and contrast (identically for compared image sets).

### Flow cytometry

Infected bacteria were analysed by flow cytometry using a NovoCyte ACEA flow cytometer (excitation laser wavelength: 561 nm, emission filter: 615/20 nm). Gates were drawn using SSC-A/FSC-A and multiple cells were excluded with SSC-H/SSC-A. Uninfected cells and bacteria infected by non-fluorescent phage were included as controls. Experiments were performed at least twice with similar results. Approximately 300,000 events were recorded per experiment. Analysis was done with NovoExpress version 1.6.1.

### Ziehl-Neelsen staining

Concentrated cultures were fixed on glass slides by heating at 150 °C for 15 min, followed by chemical fixation with methanol. BD Carbolfuchsin kit was used following the manufacturer's instructions. Samples were observed using an Evos M7000 imaging system.

### Drug susceptibility testing

The Clinical and Laboratory Standards Institute guidelines<sup>49</sup> were followed to determine the MICs. Briefly, all cultures were incubated in cation-adjusted Mueller–Hinton Broth (Merck, 90922) at 30 °C prior to the experiment. Each well of a 96-well plate was filled with 100 μl of bacterial suspension previously inoculated with 5 × 10<sup>6</sup> c.f.u. ml<sup>-1</sup>, except for the first column, to which 198 μl of the bacterial suspension was added. Drug (2 μl) at its highest concentration was added to the first column containing 198 μl of bacterial suspension and was twofold serially diluted. Results were obtained after 4 d of incubation at 30 °C without agitation. Three independent experiments were carried out in duplicate.

### Statistical analysis

Statistical analysis was carried out with GraphPad Prism v.9.0.0 for Windows. Descriptive statistics are cited and represented as median and interquartile range for each of the variables calculated. A non-parametric Dunn's test was used to compare the different conditions at 48 h for *M. smegmatis* or 144 h for *M. abscessus*. An a priori significance level was set at  $\alpha = 0.05$ .

### Phylogenetic analysis of TPP pathway amino acid sequences in *M. abscessus*

A phylogenetic tree was constructed for a concatenated alignment of amino acid sequences of the five TPP synthesis pathway members for 143 clinical isolates of *M. abscessus* and *M. abscessus* ATCC19977. Homologues were identified using MMSeqs2 (v.13.45111) and phammseqs (v.1.0.4)<sup>50</sup> and subsequently aligned using ClustalO (v.1.2.4) and Trimal (v.1.4.1)<sup>51</sup>. A concatenated alignment was generated with a custom Python script and the maximum-likelihood phylogeny was generated using RAxML (v.8.2.12)<sup>52</sup>.

### Reporting summary

Further information on research design is available in the Nature Portfolio Reporting Summary linked to this article.

### Data availability

The genome sequences of mycobacteriophages referenced here are available at [phagesdb.org](https://phagesdb.org). The genome sequences of the *M. abscessus* strains are available at <https://osf.io/hjb7q/> and at NCBI BioProject PRJNA669041. All biological materials described in this study are available from G.F.H. at [gfh@pitt.edu](mailto:gfh@pitt.edu) on reasonable request.

## References

1. Martiniano, S. L., Nick, J. A. & Daley, C. L. Nontuberculous mycobacterial infections in cystic fibrosis. *Thorac. Surg. Clin.* **29**, 95–108 (2019).
2. Johansen, M. D., Herrmann, J. L. & Kremer, L. Non-tuberculous mycobacteria and the rise of *Mycobacterium abscessus*. *Nat. Rev. Microbiol.* **18**, 392–407 (2020).
3. Nick, J. A., Daley, C. L., Lenhart-Pendergrass, P. M. & Davidson, R. M. Nontuberculous mycobacteria in cystic fibrosis. *Curr. Opin. Pulm. Med.* **27**, 586–592 (2021).
4. Dedrick, R. M. et al. Engineered bacteriophages for treatment of a patient with a disseminated drug-resistant *Mycobacterium abscessus*. *Nat. Med.* **25**, 730–733 (2019).
5. Dedrick, R. M. et al. Phage therapy of *Mycobacterium* infections: compassionate-use of phages in twenty patients with drug-resistant mycobacterial disease. *Clin. Infect. Dis.* **76**, 103–112 (2023).
6. Nick, J. A. et al. Host and pathogen response to bacteriophage engineered against *Mycobacterium abscessus* lung infection. *Cell* **185**, 1860–1874.e12 (2022).
7. Little, J. S. et al. Bacteriophage treatment of disseminated cutaneous *Mycobacterium chelonae* infection. *Nat. Commun.* **13**, 2313 (2022).
8. Hatfull, G. F. Mycobacteriophages: from Petri dish to patient. *PLoS Pathog.* **18**, e1010602 (2022).
9. Dedrick, R. M. et al. *Mycobacterium abscessus* strain morphotype determines phage susceptibility, the repertoire of therapeutically useful phages, and phage resistance. *mBio* **12**, e03431-20 (2021).
10. Hatfull, G. F., Dedrick, R. M. & Schooley, R. T. Phage therapy for antibiotic-resistant bacterial infections. *Annu. Rev. Med.* **73**, 197–211 (2022).
11. Hatfull, G. F. Actinobacteriophages: genomics, dynamics, and applications. *Annu. Rev. Virol.* **7**, 37–61 (2020).
12. Chen, J. et al. Defects in glycopeptidolipid biosynthesis confer phage I3 resistance in *Mycobacterium smegmatis*. *Microbiology* **155**, 4050–4057 (2009).
13. Russell, D. A. & Hatfull, G. F. PhagesDB: the actinobacteriophage database. *Bioinformatics* **33**, 784–786 (2017).
14. Pedulla, M. L. et al. Origins of highly mosaic mycobacteriophage genomes. *Cell* **113**, 171–182 (2003).
15. Pope, W. H. et al. Whole genome comparison of a large collection of mycobacteriophages reveals a continuum of phage genetic diversity. *eLife* **4**, e06416 (2015).
16. Hatfull, G. F. et al. Comparative genomic analysis of 60 mycobacteriophage genomes: genome clustering, gene acquisition, and gene size. *J. Mol. Biol.* **397**, 119–143 (2010).
17. Hatfull, G. F. et al. Exploring the mycobacteriophage metaproteome: phage genomics as an educational platform. *PLoS Genet.* **2**, e92 (2006).
18. Hatfull, G. F. Molecular genetics of mycobacteriophages. *Microbiol. Spectr.* **2**, 1–36 (2014).
19. Jacobs-Sera, D. et al. On the nature of mycobacteriophage diversity and host preference. *Virology* **434**, 187–201 (2012).
20. Guerrero-Bustamante, C. A., Dedrick, R. M., Garland, R. A., Russell, D. A. & Hatfull, G. F. Toward a phage cocktail for tuberculosis: susceptibility and tuberculocidal action of mycobacteriophages against diverse *Mycobacterium tuberculosis* strains. *mBio* **12**, e00973-21 (2021).
21. Abrahams, K. A. & Besra, G. S. Synthesis and recycling of the mycobacterial cell envelope. *Curr. Opin. Microbiol.* **60**, 58–65 (2021).
22. Gutierrez, A. V., Viljoen, A., Ghigo, E., Herrmann, J. L. & Kremer, L. Glycopeptidolipids, a double-edged sword of the *Mycobacterium abscessus* complex. *Front. Microbiol.* **9**, 1145 (2018).
23. Bernut, A. et al. Insights into the smooth-to-rough transitioning in *Mycobacterium bolletii* unravels a functional Tyr residue conserved in all mycobacterial MmpL family members. *Mol. Microbiol.* **99**, 866–883 (2016).
24. Burbaud, S. et al. Trehalose polyphleates are produced by a glycolipid biosynthetic pathway conserved across phylogenetically distant mycobacteria. *Cell Chem. Biol.* **23**, 278–289 (2016).
25. Llorens-Fons, M. et al. Trehalose polyphleates, external cell wall lipids in *Mycobacterium abscessus*, are associated with the formation of clumps with cording morphology, which have been associated with virulence. *Front. Microbiol.* **8**, 1402 (2017).
26. Thouvenel, L. et al. The final assembly of trehalose polyphleates takes place within the outer layer of the mycobacterial cell envelope. *J. Biol. Chem.* **295**, 11184–11194 (2020).
27. Hatfull, G. F. Phage therapy for nontuberculous mycobacteria: challenges and opportunities. *Pulm. Ther.* **9**, 91–107 (2023).
28. Dedrick, R. M. et al. Mycobacteriophage ZoeJ: a broad host-range close relative of mycobacteriophage TM4. *Tuberculosis* **115**, 14–23 (2019).
29. Sampson, T. et al. Mycobacteriophages BPs, Angel and Halo: comparative genomics reveals a novel class of ultra-small mobile genetic elements. *Microbiology* **155**, 2962–2977 (2009).
30. Johansen, M. D. et al. Mycobacteriophage-antibiotic therapy promotes enhanced clearance of drug-resistant *Mycobacterium abscessus*. *Dis. Model. Mech.* **14**, dmm049159 (2021).
31. Wetzel, K. S. et al. CRISPY-BRED and CRISPY-BRIP: efficient bacteriophage engineering. *Sci. Rep.* **11**, 6796 (2021).
32. Akusobi, C. et al. Transposon mutagenesis in *Mycobacterium abscessus* identifies an essential penicillin-binding protein involved in septal peptidoglycan synthesis and antibiotic sensitivity. *eLife* **11**, e71947 (2022).
33. Rifat, D., Chen, L., Kreiswirth, B. N. & Nuermberger, E. L. Genome-wide essentiality analysis of *Mycobacterium abscessus* by saturated transposon mutagenesis and deep sequencing. *mBio* **12**, e0104921 (2021).
34. Grzegorzewicz, A. E. et al. Inhibition of mycolic acid transport across the *Mycobacterium tuberculosis* plasma membrane. *Nat. Chem. Biol.* **8**, 334–341 (2012).
35. Dulberger, C. L. et al. Mycobacterial nucleoid-associated protein Lsr2 is required for productive mycobacteriophage infection. *Nat. Microbiol.* **8**, 695–710 (2023).
36. Judd, J. A. et al. A mycobacterial systems resource for the research community. *mBio* **12**, e02401–e02420 (2021).
37. Vassallo, C. N., Doering, C. R., Littlehale, M. L., Teodoro, G. I. C. & Laub, M. T. A functional selection reveals previously undetected anti-phage defence systems in the *E. coli* pangenome. *Nat. Microbiol.* **7**, 1568–1579 (2022).
38. Anantharaman, V., Makarova, K. S., Burroughs, A. M., Koonin, E. V. & Aravind, L. Comprehensive analysis of the HEPN superfamily: identification of novel roles in intra-genomic conflicts, defense, pathogenesis and RNA processing. *Biol. Direct* **8**, 15 (2013).
39. Makarova, K. S., Wolf, Y. I. & Koonin, E. V. Comparative genomics of defense systems in archaea and bacteria. *Nucleic Acids Res.* **41**, 4360–4377 (2013).
40. Touchette, M. H. et al. The rv1184c locus encodes Chp2, an acyltransferase in *Mycobacterium tuberculosis* polyacyltrehalose lipid biosynthesis. *J. Bacteriol.* **197**, 201–210 (2015).
41. McKitterick, A. C. & Bernhardt, T. G. Phage resistance profiling identifies new genes required for biogenesis and modification of the corynebacterial cell envelope. *eLife* **11**, e79981 (2022).
42. Bohm, K. et al. Genes affecting progression of bacteriophage P22 infection in *Salmonella* identified by transposon and single gene deletion screens. *Mol. Microbiol.* **108**, 288–305 (2018).

43. Mutalik, V. K. et al. High-throughput mapping of the phage resistance landscape in *E. coli*. *PLoS Biol.* **18**, e3000877 (2020).
44. Kortright, K. E., Chan, B. K. & Turner, P. E. High-throughput discovery of phage receptors using transposon insertion sequencing of bacteria. *Proc. Natl Acad. Sci. USA* **117**, 18670–18679 (2020).
45. Ko, C. C. & Hatfull, G. F. Mycobacteriophage Fruitloop gp52 inactivates Wag31 (DivIVA) to prevent heterotypic superinfection. *Mol. Microbiol.* **108**, 443–460 (2018).
46. Nesbit, C. E., Levin, M. E., Donnelly-Wu, M. K. & Hatfull, G. F. Transcriptional regulation of repressor synthesis in mycobacteriophage L5. *Mol. Microbiol.* **17**, 1045–1056 (1995).
47. Gordon, D., Abajian, C. & Green, P. Consed: a graphical tool for sequence finishing. *Genome Res.* **8**, 195–202 (1998).
48. Russell, D. A. Sequencing, assembling, and finishing complete bacteriophage genomes. *Methods Mol. Biol.* **1681**, 109–125 (2018).
49. Woods, G. L. et al. *Susceptibility Testing of Mycobacteria, Nocardiae, and Other Aerobic Actinomycetes* 2nd edn. Report no. M24-A2 (Wayne (PA): Clinical and Laboratory Standards Institute, 2011).
50. Gauthier, C. H., Cresawn, S. G. & Hatfull, G. F. PhaMMseqs: a new pipeline for constructing phage gene families using MMseqs2. *G3* **12**, jkac233 (2022).
51. Capella-Gutierrez, S., Silla-Martinez, J. M. & Gabaldon, T. trimAl: a tool for automated alignment trimming in large-scale phylogenetic analyses. *Bioinformatics* **25**, 1972–1973 (2009).
52. Stamatakis, A., Ludwig, T. & Meier, H. RAXML-III: a fast program for maximum likelihood-based inference of large phylogenetic trees. *Bioinformatics* **21**, 456–463 (2005).
53. Bachmann, B. O. & Ravel, J. Chapter 8. Methods for in silico prediction of microbial polyketide and nonribosomal peptide biosynthetic pathways from DNA sequence data. *Methods Enzymol.* **458**, 181–217 (2009).
54. Snapper, S. B., Melton, R. E., Mustafa, S., Kieser, T. & Jacobs, W. R. Jr. Isolation and characterization of efficient plasmid transformation mutants of *Mycobacterium smegmatis*. *Mol. Microbiol.* **4**, 1911–1919 (1990).

## Acknowledgements

We thank C. Akusobi, M. Sullivan, K. McGowen, C. Rodriguez, W. DePas and W. Daher for helpful discussions; all of the students and faculty in the SEA-PHAGES programme, who discovered and characterized phages used in this study; and the numerous colleagues who provided *M. abscessus* strains in the GDxx series. Microscopy and flow cytometry were performed at the Montpellier Imaging Center for Microscopy (MRI). This work was supported by grants from the National Institutes of Health (GM131729) and the Howard Hughes Medical Institute (Grant GT12053) to G.F.H., a Cystic Fibrosis Foundation Postdoc Fellowship WETZEL21F0 to K.S.W., grants from the French National Research Agency ANR-21-CE44-0027-01 (MYCOLT) to L.K. and C.C., and Vaincre la Mucoviscidose (RF20200502678) and Association Grégory Lemarchal PhD fellowship to M.I.

## Author contributions

K.S.W., M.I., G.F.H. and L.K. conceptualized the project; K.S.W., M.I., L.A., H.G.A., M.C., S.M., R.A.G. and D.A.R. conducted the investigations; K.S.W., M.I., G.F.H. and L.K. wrote the original draft; K.S.W., M.I., L.A., H.G.A., M.C., S.M., R.A.G., D.A.R., C.C., G.F.H. and L.K. reviewed and edited the manuscript; K.S.W., M.I., G.F.H. and L.K. acquired funding; and G.F.H. and L.K. supervised the project.

## Competing interests

GFH receives support through a Collaborative Research Agreement with Janssen Inc., which did not fund the work reported here. The remaining authors declare no competing interests.

## Additional information

**Extended data** is available for this paper at <https://doi.org/10.1038/s41564-023-01451-6>.

**Supplementary information** The online version contains supplementary material available at <https://doi.org/10.1038/s41564-023-01451-6>.

**Correspondence and requests for materials** should be addressed to Graham F. Hatfull or Laurent Kremer.

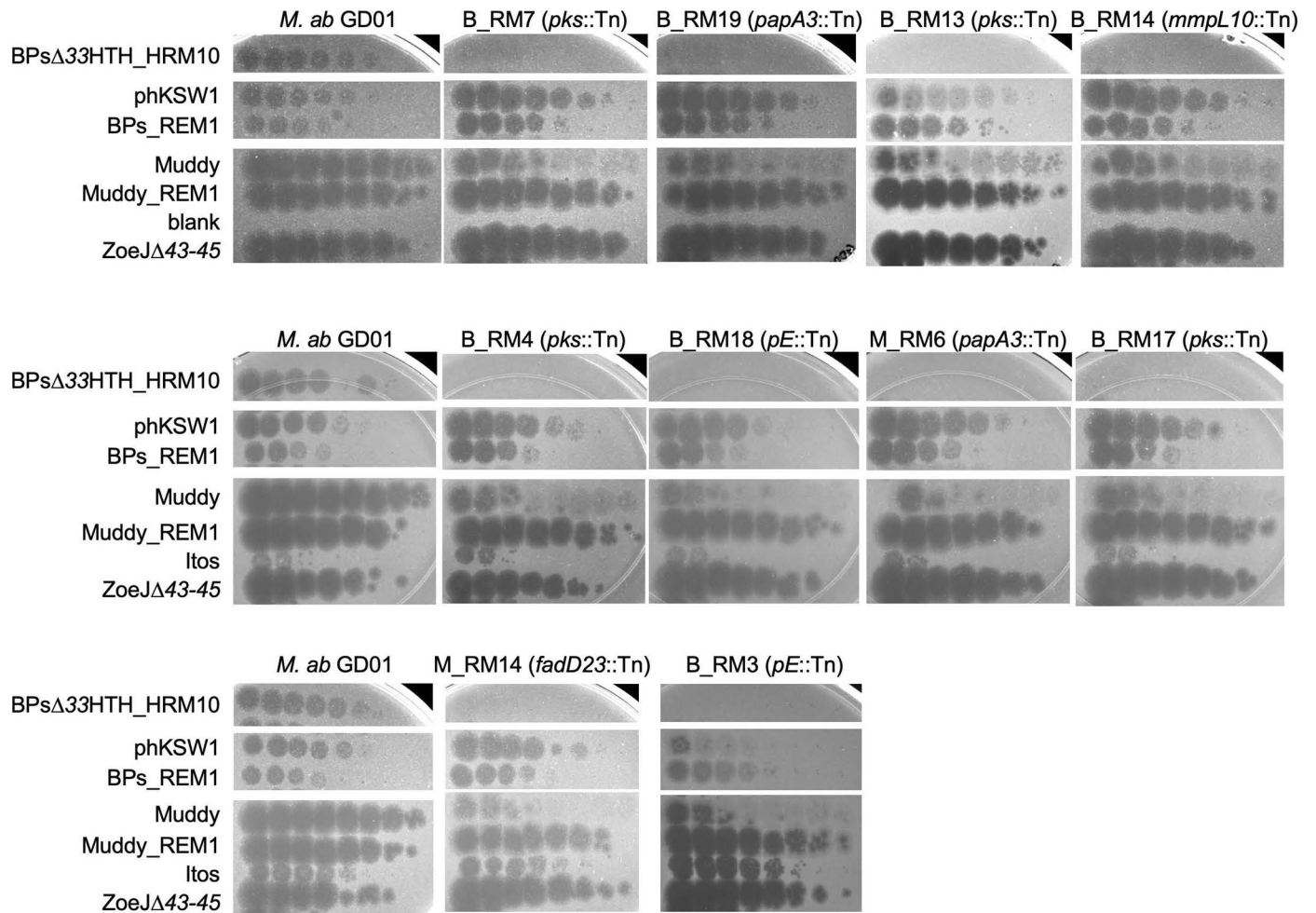
**Peer review information** *Nature Microbiology* thanks Jeremy Rock, William Jacobs and the other, anonymous, reviewer(s) for their contribution to the peer review of this work.

**Reprints and permissions information** is available at [www.nature.com/reprints](http://www.nature.com/reprints).

**Publisher's note** Springer Nature remains neutral with regard to jurisdictional claims in published maps and institutional affiliations.

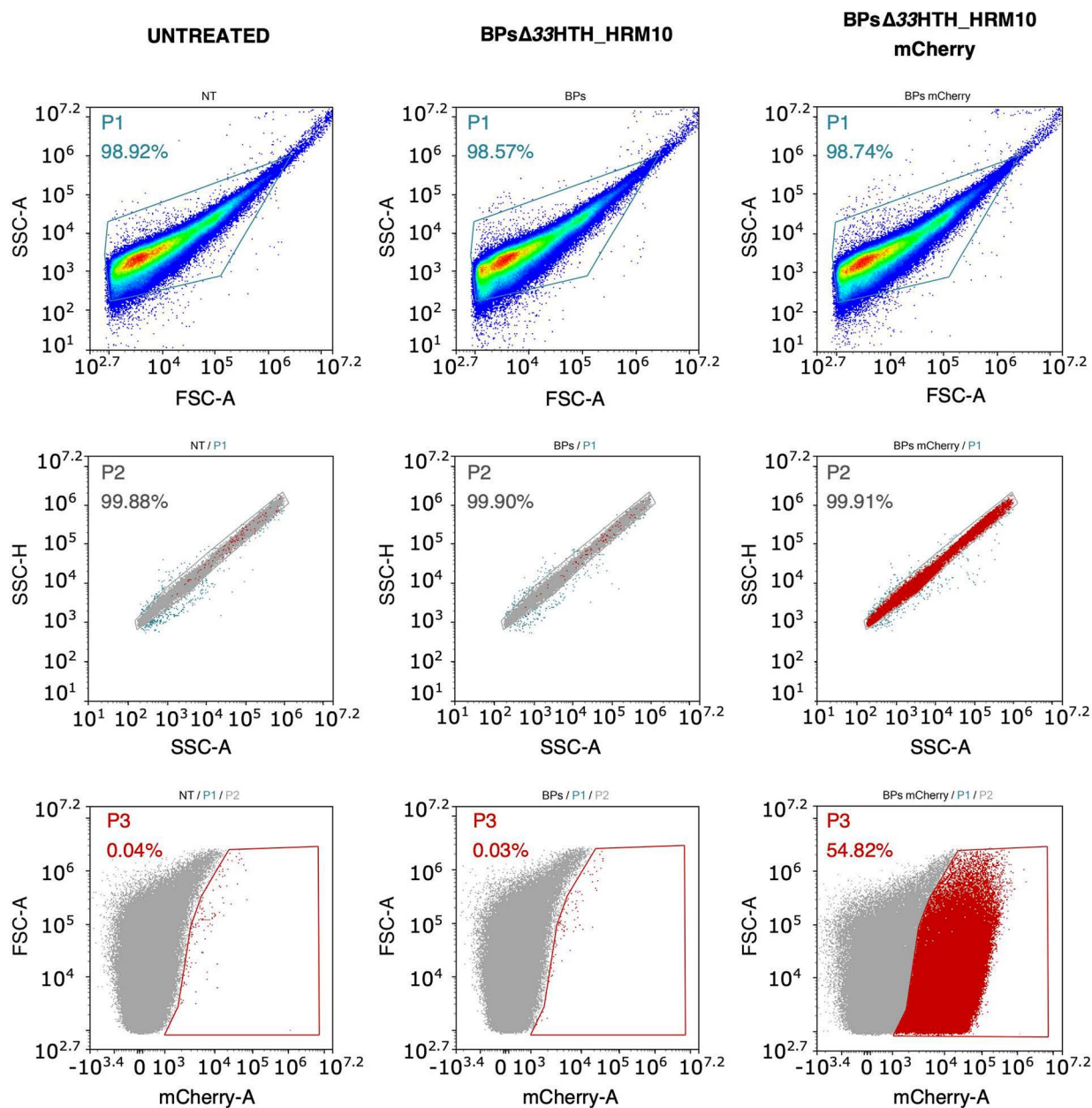
**Open Access** This article is licensed under a Creative Commons Attribution 4.0 International License, which permits use, sharing, adaptation, distribution and reproduction in any medium or format, as long as you give appropriate credit to the original author(s) and the source, provide a link to the Creative Commons license, and indicate if changes were made. The images or other third party material in this article are included in the article's Creative Commons license, unless indicated otherwise in a credit line to the material. If material is not included in the article's Creative Commons license and your intended use is not permitted by statutory regulation or exceeds the permitted use, you will need to obtain permission directly from the copyright holder. To view a copy of this license, visit <http://creativecommons.org/licenses/by/4.0/>.

© The Author(s) 2023



**Extended Data Fig. 1 | Plaque assays of phages on *M. abscessus* GD01 transposon insertion mutants.** Phages as shown on the left were spotted onto solid media with *M. abscessus* GD01 or transposon insertion mutant strains. Each row indicates a set strains tested together.

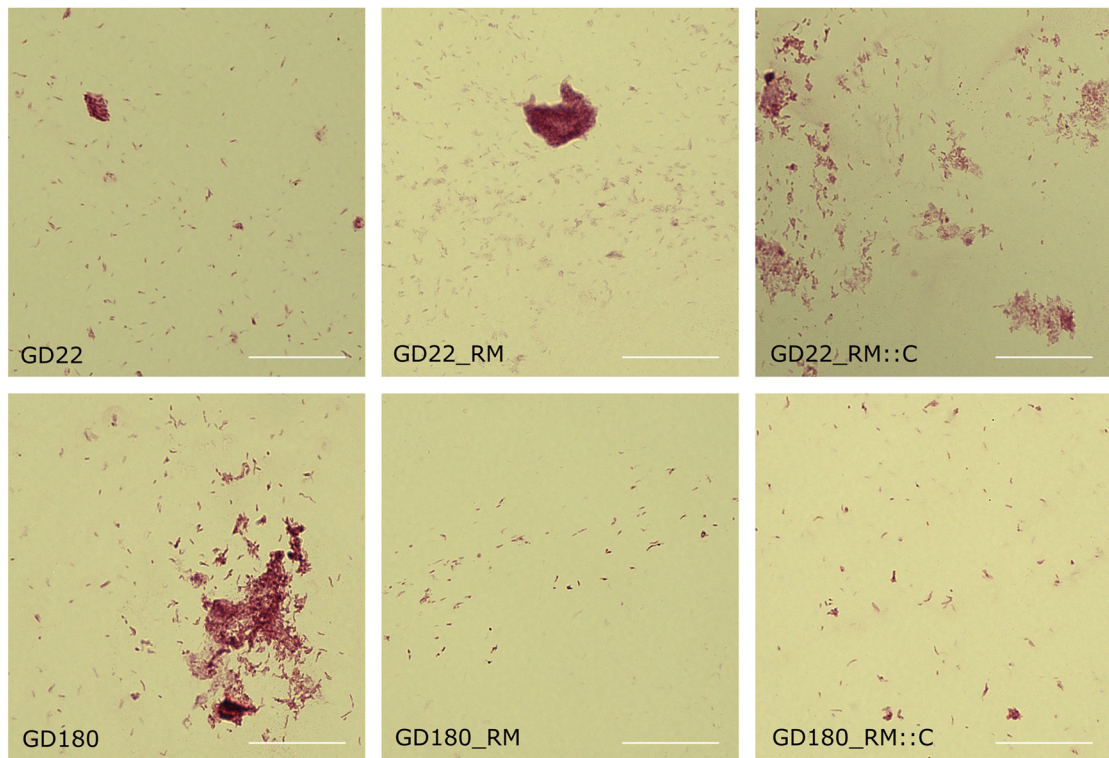




**Extended Data Fig. 2 | Gating strategy for flow cytometry analysis of fluorophage-infected bacteria.** Bacteria untreated or infected with non-fluorescent phages were used as controls. The first gate was plotted on SSC-A/FSC-A to exclude cellular debris. SSC-H/SSC-A was analysed to

eliminate multiple cells. The gate for fluorescence was drawn thanks to controls to exclude non-fluorescent bacteria. The analysis was performed on approximately 300,000 bacteria using NovoExpress software. Here is shown an example of analysis for GD22 strain performed at least twice.

A



B

Strains		MIC (µg/mL) <sup>a</sup>								
		AMK	IPM	BDQ	RFB	CFZ	LNZ	CFX	ZEO	AU1235
GD22	Exp 1	25	25-50	0.098	12.5	3.125	12.5	50-100	12.5	0.39
	Exp 2	50	50	0.098	25	1.56	25	100	12.5	0.195
	Exp 3	100	50	0.098	25	0.39	6.25	100	6.25	0.39
GD22_RM4	Exp 1	25	25	0.195	12.5	1.56	6.25	50	6.25	0.78
	Exp 2	50	25	0.098	12.5	1.56	12.5	50	6.25	0.195
	Exp 3	50	100	0.098	25	3.25	12.5	50	12.5	0.195
GD22_RM4 :: C	Exp 1	50	12.5	0.098	12.5	1.56	12.5	50	6.25	0.39
	Exp 2	50	25	0.098	12.5	0.78	12.5	50	6.25	0.195
	Exp 3	50	25-50	0.19	25	1.56	6.25	50	6.25	0.195
GD180	Exp 1	25	25	0.098	1.56	ND	12.5	25	>200	0.048
	Exp 2	25	50	0.048	6.25	0.78	6.25	50	>200	<0.048
	Exp 3	50	25	0.024	12.5	0.78	6.25	25	>200	0.19
GD180_RM2	Exp 1	25	12.5	0.024	3.125	1.56	6.25	25	>200	0.39
	Exp 2	50	25	0.098	3.125	1.56	1.56	25	>200	<0.048
	Exp 3	50	12.5	0.048	6.25	0.78	1.56	25	>200	0.19
GD180_RM2 :: C	Exp 1	50	25	0.098	3.125	0.78	3.125	25	>200	0.098
	Exp 2	25	50	0.024	3.125	0.78	3.125	50	>200	<0.048
	Exp 3	50	25	0.024	3.125	0.78	3.125	25	>200	0.098
CIP104536 (R)	Exp 1	50	50	0.048	12.5-25	1.56	25	100	50	0.39
	Exp 2	50	25	0.098	25	0.78	12.5	50	25	0.78

<sup>a</sup> MICs (µg/ml) were determined following the CLSI guidelines.

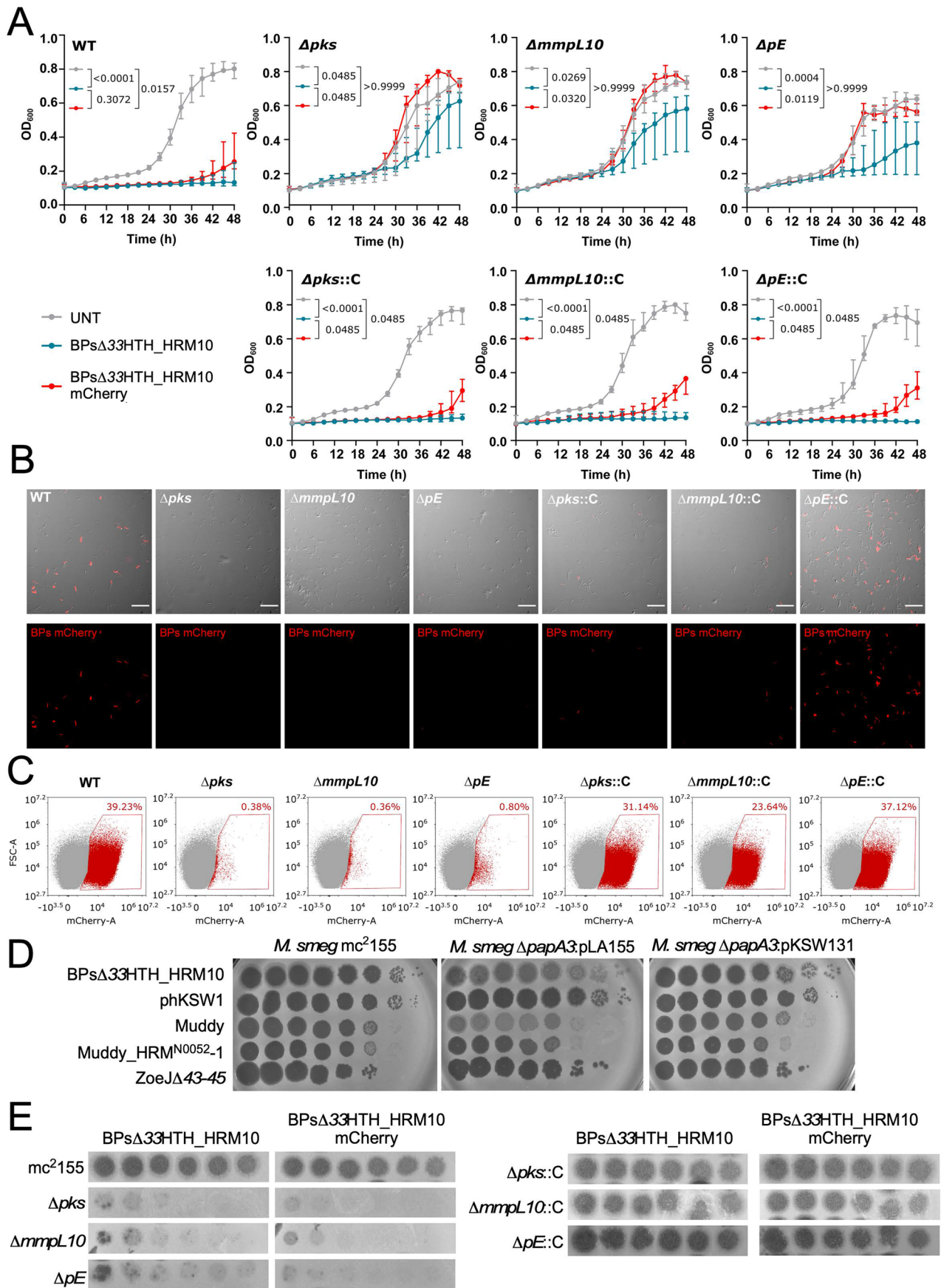
AMK, amikacin; IPM, imipenem; BDQ, bedaquiline; RFB, rifabutin; CFZ, clofazimine; LNZ, linezolid; CFX, ceftiofloxacin; ZEO, zeocin; AU1235, MmpL3 inhibitor

Extended Data Fig. 3 | See next page for caption.

**Extended Data Fig. 3 | Characterization of TPP-defective mutants.**

**A.** Ziehl-Neelsen staining of *M. abscessus* TPP mutants. Cultures of GD22, GD22\_RM, GD22\_RM::C, GD180, GD180\_RM and GD180\_RM::C were fixed on glass slides and acid-fast staining was performed using the BD Carbofuchsin kit, and observed microscopically at 60x magnification. This assay was performed three times. Scale bar: 30  $\mu\text{m}$ . **B.** MIC (in  $\mu\text{g}/\text{mL}$ ) values of antibiotics determined in

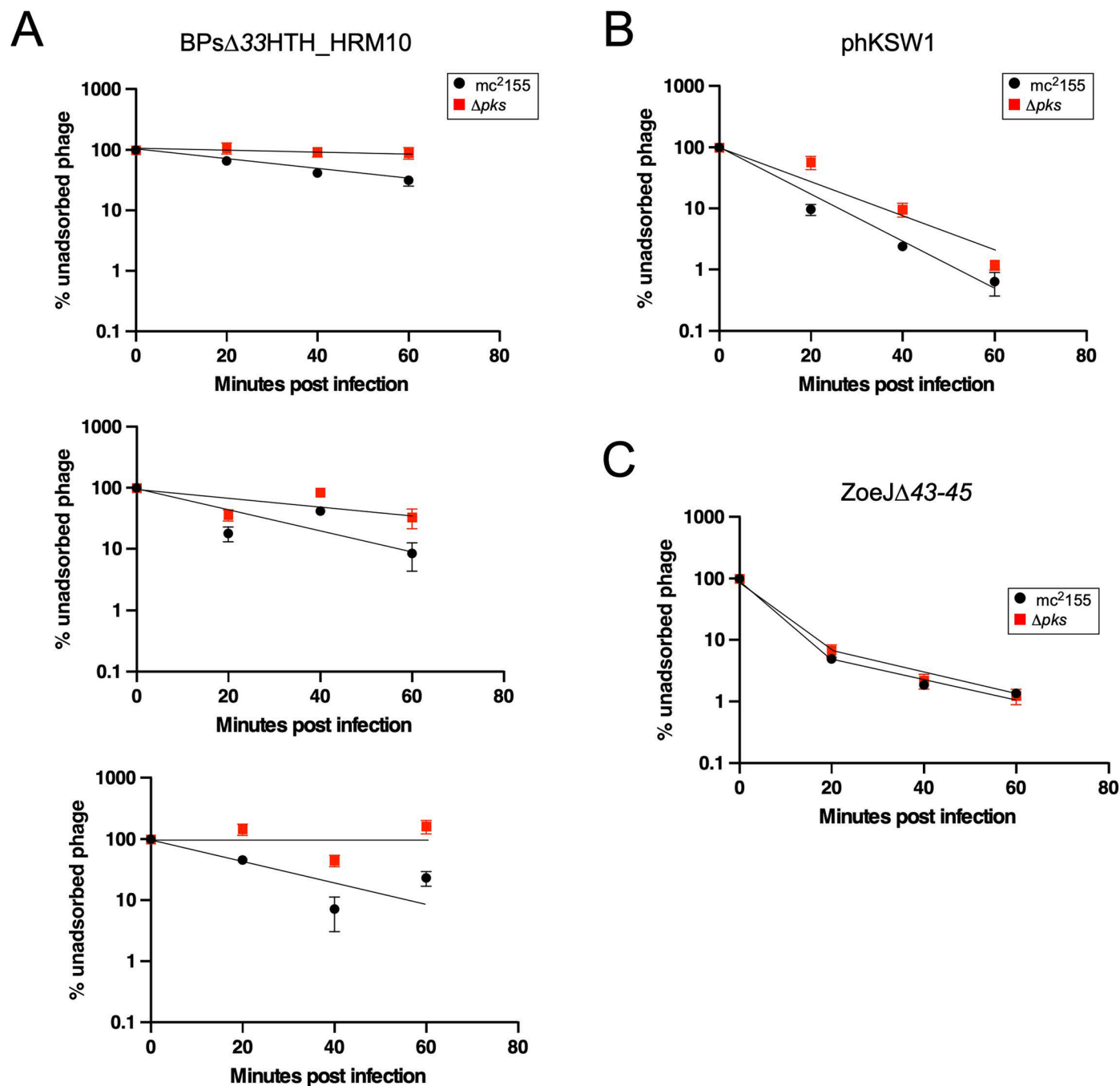
Cation-adjusted Mueller-Hinton Broth (CaMHB) at 30 °C against *M. abscessus* clinical isolates (GD22 and GD180), resistant mutants (GD22\_RM4 and GD180\_RM2) and complemented strains (GD22\_RM4::C and GD180\_RM2::C) with CIP104536 (ATCC19977) as a control. Results from three independent experiments are shown.



Extended Data Fig. 4 | See next page for caption.

**Extended Data Fig. 4 | Infection of *M. smegmatis* TPP mutants by BPs and its derivatives. A.** Growth curves of the different strains incubated with phage BPs $\Delta$ 33HTH\_HRM10 or BPs $\Delta$ 33HTH\_HRM10-mCherry at MOI 10 or without (UNT) for 2 days in 7H9/OADC supplemented with 1 mM CaCl<sub>2</sub> at 37 °C without agitation. Measurements were taken every 3 hours. Data shown are represented as median of three independent experiments done in triplicate  $\pm$  interquartile range. Two-sided Dunn's multiple comparisons test was used to perform statistical analysis. Statistical analysis was done to compare the differences at 48 hours between each strain, p values are mentioned on each plot. **B.** Representative microscope fields of *M. smegmatis* strains infected with the fluorophage BPs $\Delta$ 33HTH\_HRM10-mCherry (designated BPs mCherry) (MOI 10) for 2 hours at 37 °C. Similar results

were obtained at least three times. Scale bars: 30  $\mu$ m. **C.** Flow cytometry data plotted as a dot plot showing the percentage of bacilli infected with BPs $\Delta$ 33HTH\_HRM10-mCherry relative to the study population. This assay was conducted twice with similar results obtained. **D.** Phage infection of *M. smegmatis* TPP mutants. Phages as shown on the left were tenfold serially diluted and spotted onto solid media with *M. smegmatis* mc<sup>2</sup>155, *M. smegmatis*  $\Delta$ papA3:pLAI55 or *M. smegmatis*  $\Delta$ papA3:pKSW131. **E.** Plaquing of BPs $\Delta$ 33HTH\_HRM10 and the mCherry derivative on *M. smegmatis* strains defective in TPP production (left panels) and the complemented strains (right panels). Phage lysates were tenfold serially diluted prior to spotting on bacterial lawns. Similar results were obtained at least three times and a representative experiment is shown.



**Extended Data Fig. 5 | Additional replicates of phage adsorption assays on *M. smegmatis* mc<sup>2</sup>155 and  $\Delta$ pks.** Biological replicates of phage adsorption assays for phages BPs $\Delta$ 33HTH\_HRM10 (A), phKSW1 (B) and ZoeJ $\Delta$ 43-45 (C) are shown. Data are represented as the mean of technical duplicates  $\pm$  SD. For

BPs $\Delta$ 33HTH\_HRM10, each individual assay showed reduced adsorption on  $\Delta$ pks as compared to mc<sup>2</sup>155. However, the measured adsorption rates varied between each replicate, such that observed differences were obfuscated when displaying the means; representative replicates for all phages are shown in Fig. 5.

Extended Data Table 1 | Characterization of phage resistant *M. abscessus* GD01 transposon mutants

Strain Name <sup>1</sup>	Isolated as resistant to <sup>2</sup>	# Insert <sup>3</sup>	Tn insertion coordinate <sup>4</sup>	Tn Dir <sup>5</sup>	GD01 Locus Tag <sup>6</sup>	ATCC19977 Gene <sup>7</sup>	Protein <sup>8</sup>	PCR ver. <sup>9</sup>	Plaque assay <sup>10</sup>
GD01Tn_Muddy_RM9	Muddy	≥1	895811	Rev	EXM25_04535	MAB_0935c	FadD23	Y	Y
GD01Tn_BPsHRM10_RM9	BPs_HRM10	≥1	896103	Fwd	EXM25_04535	MAB_0935c	FadD23	ND	ND
GD01Tn_BPsHRM10_RM15	BPs_HRM10	≥1	896250	Rev	EXM25_04535	MAB_0935c	FadD23	ND	ND
GD01Tn_Muddy_RM14	Muddy	≥2	#1 896251 #2 2068078	Fwd Fwd	EXM25_04535 EXM25_10305	MAB_0935c MAB_2130	FadD23 HAD	Y Y	Y Y
GD01Tn_Muddy_RM11 <sup>11</sup>	Muddy	≥1	896372	Rev	EXM25_04535	MAB_0935c	FadD23	ND	ND
GD01Tn_Muddy_RM15 <sup>11</sup>	Muddy	≥1	896372	Rev	EXM25_04535	MAB_0935c	FadD23	ND	ND
GD01Tn_Muddy_RM13	Muddy	≥1	896513	Rev	EXM25_04535	MAB_0935c	FadD23	ND	ND
GD01Tn_Muddy_RM7	Muddy	≥1	896840	Rev	EXM25_04535	MAB_0935c	FadD23	ND	ND
GD01Tn_Muddy_RM12	Muddy	≥1	896990	Rev	EXM25_04535	MAB_0935c	FadD23	Y	Y
GD01Tn_BPsHRM10_RM1	BPs_HRM10	≥1	897275	Rev	EXM25_04535	MAB_0935c	FadD23	Y	Y
GD01Tn_BPsHRM10_RM6	BPs_HRM10	≥1	897828	Rev	EXM25_04540	MAB_0936c	PE	Y	Y
GD01Tn_BPsHRM10_RM3	BPs_HRM10	≥2	#1 898266 #2 1702803	Fwd Rev	EXM25_04540 EXM25_08515	MAB_0936c MAB_1681	PE Hyp	Y Y	Y Y
GD01Tn_BPsHRM10_RM8	BPs_HRM10	≥2	#1 898475 #2 2710182	Fwd Rev	EXM25_04540 EXM25_13435	MAB_0936c MAB_2752	PE ABC	ND ND	ND ND
GD01Tn_Muddy_RM20	Muddy		898646	Rev	EXM25_04540	MAB_0936c	PE	Y	Y
GD01Tn_BPsHRM10_RM18	BPs_HRM10	≥2	#1 898656 #2 50130	Rev Fwd	EXM25_04540 EXM25_00255	MAB_0936c MAB_0457	PE Hyp	Y Y	Y Y
GD01Tn_BPsHRM10_RM20	BPs_HRM10	≥3	#1 899155 #2 2314064 #3 4430814	Fwd Fwd Fwd	EXM25_04545 EXM25_11400 Inter EXM25_22125-22130	MAB_0937c MAB_2352 MAB_4446-4447	Mmpl10 DNA glyc Hyp/ABC	ND ND ND	ND ND ND
GD01Tn_BPsHRM10_RM11	BPs_HRM10	≥1	899212	Fwd	EXM25_04545	MAB_0937c	Mmpl10	Y	Y
GD01Tn_BPsHRM10_RM14	BPs_HRM10	≥2	#1 900526 #2 3419195	Rev Rev	EXM25_04545 EXM25_17025	MAB_0937c MAB_3426c	Mmpl10 SDR	Y Y	Y Y
GD01Tn_BPsHRM10_RM19	BPs_HRM10	≥2	#1 901936 #2 2004769	Fwd Rev	EXM25_04550 EXM25_10050	MAB_0938c MAB_2081	PapA3 Acyl-CoA	Y Y	Y Y
GD01Tn_BPsHRM10_RM2	BPs_HRM10	≥1	901937	Rev	EXM25_04550	MAB_0938c	PapA3	ND	ND
GD01Tn_Muddy_RM17	Muddy	≥1	902798	Fwd	EXM25_04550	MAB_0938c	PapA3	Y	Y
GD01Tn_BPsHRM10_RM10	BPs_HRM10	≥1	902799	Rev	EXM25_04550	MAB_0938c	PapA3	Y	Y
GD01Tn_Muddy_RM1 <sup>11</sup>	Muddy	≥2	902799 1708979	Rev Fwd	EXM25_04550 EXM25_08540	MAB_0938c MAB_1686	PapA3 Hyp	ND ND	ND ND
GD01Tn_Muddy_RM3 <sup>11</sup>	Muddy	≥2	902799 1708979	Rev Fwd	EXM25_04550 EXM25_08540	MAB_0938c MAB_1686	PapA3 Hyp	ND ND	ND ND
GD01Tn_Muddy_RM6	Muddy	≥2	#1 902802 #2 1799970	Rev Fwd	EXM25_04550 EXM25_09000	MAB_0938c MAB_1882c	PapA3 DoxX	Y Y	Y Y
GD01Tn_Muddy_RM19	Muddy		903001	Rev	EXM25_04550	MAB_0938c	PapA3	Y	Y
GD01Tn_BPsHRM10_RM4	BPs_HRM10	≥2	#1 903920 #2 3438375	Fwd Fwd	EXM25_04555 EXM25_17140	MAB_0939 MAB_3449c	MFS	Y Y	Y Y
GD01Tn_BPsHRM10_RM5	BPs_HRM10	≥2	#1 905614 #2 3575341	Fwd Fwd	EXM25_04555 EXM25_17815	MAB_0939 MAB_3593	Pks MgtC	Y Y	Y Y
GD01Tn_BPsHRM10_RM17	BPs_HRM10	≥2	#1 911720 #2 3319297	Rev Rev	EXM25_04555 EXM25_16510	MAB_0939 MAB_3332c	Pks DoxX	Y Y	Y Y
GD01Tn_BPsHRM10_RM13	BPs_HRM10	≥2	#1 914389 #2 934573	Fwd Rev	EXM25_04555 EXM25_04650	MAB_0939 MAB_0958c	Pks NAD(P)	Y Y	Y Y
GD01Tn_BPsHRM10_RM7	BPs_HRM10	≥2	#1 914477 #2 3546108	Rev Rev	EXM25_04555 Inter EXM25_17670-17675	MAB_0939 MAB_3538-3539	Pks Kinase/ WhiB	Y Y	Y Y
GD01Tn_phKSW1_RM1 <sup>11</sup>	phKSW1	1	1711653	Fwd	EXM25_08560	MAB_1690	ABC	Y	Y
GD01Tn_phKSW1_RM4 <sup>11</sup>	phKSW1	1	1711653	Fwd	EXM25_08560	MAB_1690	ABC	Y	Y
GD01Tn_phKSW1_RM2	phKSW1	1	1169901	Fwd	Inter EXM25_05825-05830	None – MAB_1175	DUF4145	Y	Y
GD01Tn_phKSW1_RM7 <sup>11</sup>	phKSW1	≥2	#1 1169901 #2 2201133	Fwd Fwd	Inter EXM25_05825-05830 EXM25_10900	None – MAB_1175 MAB_2245	DUF4145	Y Y	Y Y
GD01Tn_phKSW1_RM8 <sup>11</sup>	phKSW1	≥2	#1 1169901 #2 2201133	Fwd Fwd	Inter EXM25_05825-05830 EXM25_10900	None – MAB_1175 MAB_2245	DUF4145	Y Y	Y Y
GD01Tn_phKSW1_RM5	phKSW1	≥2	#1 1169902 #2 4426058	Rev Rev	Inter EXM25_05825-05830 EXM25_22105	None – MAB_1175 MAB_4441	DUF4145	Y Y	Y Y
GD01Tn_phKSW1_RM6	phKSW1	2	#1 3688289 #2 429116	Fwd Fwd	EXM25_18375 EXM25_02155	MAB_3698 MAB_0399c	ATP RecB	Y Y	Y Y
GD01Tn_phKSW1_RM10	phKSW1	2	#1 1708979 #2 902799	Fwd Rev	EXM25_08540 EXM25_04550	MAB_1686 MAB_0938c	Hyp PapA3	Y Y	Y Y
GD01Tn_phKSW1_RM11a	phKSW1	≥2	#1 3371296 #2 4561506	Rev Fwd	EXM25_16760 EXM25_22720	MAB_3381c MAB_4573c	Mif EphC	Y Y	Y Y
GD01Tn_MuddyREM1_RM2	Muddy_REM1	≥2	#1 1195603 #2 4785617	Rev Fwd	EXM25_05970 EXM25_23740	MAB_1201c MAB_4773	GreA HMOX	Y Y	Y Y
GD01Tn_MuddyREM1_RM3	Muddy_REM1	>1	3850846	Rev	EXM25_19265	MAB_3868c	RpoC	Y	Y

<sup>1</sup>Strain names include three parameters separated by underscores: i.e. Parent strain\_phage used for selection\_mutant number.

<sup>2</sup>The strain was isolated from a solid agar plate seeded with phages as indicated.

<sup>3</sup>The likely number of Tn insertions in each strain: ≥1 indicates that we have mapped one insertion, but we cannot exclude that there are one or more additional insertions.; ≥2 indicates that two insertions were mapped, but we cannot exclude that there are one or more additional insertions. Five phKSW1 resistant strains were whole genome sequenced such that the precise number of insertions are known, as indicated.

<sup>4</sup>Coordinates of the transposon insertions mapped in *M. abscessus* GD01 (accession number CP035923.1). Where more than one Tn has been mapped, they are listed as #1 and #2, and #2 is shown in grey shading. Strains with similar coordinates are listed together.

<sup>5</sup>Orientation of the Tn insertion, Forward (Fwd) or reverse (Rev) compared to the genome.

<sup>6</sup>The locus tag of the strain GD01 gene with the Tn insertion is shown. Intergenic insertions show the two flanking locus tags.

<sup>7</sup>The gene name of the *M. abscessus* ATCC19977 (NC\_010397.1) homolog(s) of the interrupted genes is shown. For intergenic insertions, flanking genes are shown.

<sup>8</sup>Protein names or predicted function of genes with Tn insertions are shown, or functions of flanking genes for intergenic insertions.

<sup>9</sup>The location of the transposon insertion was confirmed by a second PCR with primers designed to flank the insertion site. Y, Yes; ND, Not determined.

<sup>10</sup>The strain was streaked out to remove phage, grown in liquid media and tested for phage resistance by plaque assay. Y, Yes; ND, Not determined.

<sup>11</sup>In four instances, two strains isolated against the same phage were found to have identical transposon insertion sites and are likely siblings. GD01Tn\_phKSW1\_RM1 and GD01Tn\_phKSW1\_RM4 are likely siblings, as are GD01Tn\_phKSW1\_RM7 and GD01Tn\_phKSW1\_RM8. GD01Tn\_phKSW1\_RM2, GD01Tn\_phKSW1\_RM5, and GD01Tn\_phKSW1\_RM7 have insertions in the same location (coordinate 1169901) but are not siblings as they have Tn insertions in different orientations or different secondary insertions.

**Extended Data Table 2 | Phage BPs and Muddy mutants escaping TPP-loss mediated resistance**

Phage <sup>1</sup>	Parent <sup>2</sup>	Amino Acid Substitution <sup>3</sup>	Isolated on <sup>4</sup>	Reference
phKSW2	BPs $\Delta$ 33HTH_HRM10	gp22 L462R	<i>M. ab.</i> GD01Tn BPs_HRM10_RM6	This work
phKSW3	BPs $\Delta$ 33HTH_HRM10	gp22 A306V	<i>M. ab.</i> GD01Tn BPs_HRM10_RM6	This work
phKSW4 (Prob. a sib of phKSW2)	BPs $\Delta$ 33HTH_HRM10	gp22 L462R	<i>M. ab.</i> GD01Tn BPs_HRM10_RM11	This work
phKSW5	BPs $\Delta$ 33HTH_HRM10	gp22 A604E	<i>M. ab.</i> GD01Tn BPs_HRM10_RM11	This work
BPs_REM1	BPs $\Delta$ 33HTH_HRM10	gp22 L462R; G780R	<i>M. ab.</i> GD180_RM2	This work
phKSW1	BPs $\Delta$ 33HTH_HRM10	gp22 A604E	<i>M. smegmatis</i> $\Delta$ MSMEG_5439	This work
Muddy_REM1	Muddy	gp24 E680K	<i>M. ab.</i> GD180_RM2	This work
Muddy_HRM <sup>N0157</sup> -1	Muddy	gp24 G487W	<i>M. tuberculosis</i> N0157	Ref. 20 <sup>5</sup>
Muddy_HRM <sup>N0157</sup> -2	Muddy	gp24 T608A	<i>M. tuberculosis</i> N0157	Ref. 20 <sup>5</sup>
Muddy_HRM <sup>N0052</sup> -1	Muddy	gp24 E680K	<i>M. tuberculosis</i> N0052	Ref. 20 <sup>5</sup>

<sup>1</sup>Name of a phage able to form more clear plaques on TPP synthesis pathway mutants. <sup>2</sup>Parent phage from which the mutant was isolated. <sup>3</sup>Amino acid substitutions identified in mutant phages. <sup>4</sup>The *M. abscessus* or *M. tuberculosis* strain on which the mutant phage was isolated <sup>5</sup>Data from reference <sup>20</sup>.



**Extended Data Table 3 | *M. abscessus* mutants spontaneously resistant to phage BPs derivatives**

Resistant mutant <sup>1</sup>	Parent <sup>2</sup>	Isolated as resistant to <sup>3</sup>	Mutated gene <sup>4</sup>	Amino Acid Substitution <sup>5</sup>	Reference
GD17_RM1	<i>M. ab.</i> GD17	BPsHRM <sup>GD03</sup>	<i>pks</i>	G210V	Ref. 9 <sup>6</sup>
GD22_RM4	<i>M. ab.</i> GD22	BPsΔ33HTH_HRM10 and Itos	<i>pks</i>	W2389fsX2406	Ref. 9 <sup>6</sup>
GD38_RM2	<i>M. ab.</i> GD38	BPsΔ33HTH_HRM10	<i>pks</i>	M2115fsX2118	This work
GD59_RM1	<i>M. ab.</i> GD59	BPsΔ33HTH_HRM10 and Itos	<i>pks</i>	D327Y	This work
GD180_RM2	<i>M. ab.</i> GD180	BPsΔ33HTH_HRM10	<i>mmpL10</i>	S688fsX704	This work

<sup>1</sup>Resistant mutants were named after the parent strain and the number of the resistant mutant (RM) isolated. <sup>2</sup>Parent strain of *M. abscessus* from which the resistant mutant was isolated upon phage infection. <sup>3</sup>RMs were isolated by infecting cell cultures at a high MOI and plating infections on solid media to isolate survivors. <sup>4</sup>The entire genomes of the resistant mutants were sequenced and compared to the genomes of the parents to identify mutated genes conferring phage resistance. <sup>5</sup>The amino acid substitution in the protein product resulting from the gene mutation. <sup>6</sup>Data from reference <sup>9</sup>.

Extended Data Table 4 | List of strains used in this study

Name	Description / genotype	Reference
<i>M. smegmatis</i> (WT)	<i>M. smegmatis</i> , strain mc <sup>2</sup> 155	Ref. 54 <sup>1</sup>
$\Delta$ pks (PMM284)	<i>M. smegmatis</i> mc <sup>2</sup> 155 $\Delta$ pks::res	Ref. 24 <sup>2</sup>
$\Delta$ mmpL10 (PMM223)	<i>M. smegmatis</i> mc <sup>2</sup> 155 $\Delta$ mmpL10::res	Ref. 24 <sup>2</sup>
$\Delta$ pE (PMM229)	<i>M. smegmatis</i> mc <sup>2</sup> 155 $\Delta$ pE::res	Ref. 24 <sup>2</sup>
$\Delta$ pks::C (PMM284/pMVpks)	<i>M. smegmatis</i> mc <sup>2</sup> 155 $\Delta$ pks::res complemented with pMVpks, Hyg <sup>R</sup>	Ref. 24 <sup>2</sup>
$\Delta$ mmpL10::C (PMM223/pMVmmpL10)	<i>M. smegmatis</i> mc <sup>2</sup> 155 $\Delta$ mmpL10::res complemented with pMVmmpL10, Hyg <sup>R</sup>	Ref. 24 <sup>2</sup>
$\Delta$ pE::C (PMM229/pMVpE)	<i>M. smegmatis</i> mc <sup>2</sup> 155 $\Delta$ pE::res complemented with pMVpE, Hyg <sup>R</sup>	Ref. 24 <sup>2</sup>
GD01	<i>M. abscessus subsp. massiliense</i> , R morphotype	Ref. 4 <sup>3</sup>
fadD23::Tn :pKSW134	GD0Tn_BPsHRM10_RM1 complemented with pKSW134	This study
GD17	<i>M. abscessus subsp. abscessus</i> , R morphotype	Ref. 9 <sup>4</sup>
GD17_RM1	<i>M. abscessus subsp. abscessus</i> , R morphotype	Ref. 9 <sup>4</sup>
GD22	<i>M. abscessus subsp. abscessus</i> , R morphotype	Ref. 9 <sup>4</sup>
GD22_RM4	<i>M. abscessus subsp. abscessus</i> spontaneous resistant mutant, R morphotype	Ref. 9 <sup>4</sup>
GD22_RM4::C	<i>M. abscessus</i> GD22_RM4 complemented with pMVpks_mWasabi, Hyg <sup>R</sup>	This study
GD38	<i>M. abscessus subsp. abscessus</i> , R morphotype	Ref. 9 <sup>4</sup>
GD59_RM1	<i>M. abscessus subsp. abscessus</i> , R morphotype	Ref. 9 <sup>4</sup>
GD59	<i>M. abscessus subsp. abscessus</i> , R morphotype	Ref. 9 <sup>4</sup>
GD180	<i>M. abscessus subsp. abscessus</i> , R morphotype	This study
GD180_RM2	<i>M. abscessus subsp. abscessus</i> , spontaneous resistant mutant, R morphotype	This study
GD180_RM2::C	<i>M. abscessus</i> GD180_RM2 complemented with pMVmmpL10_mWasabi, Hyg <sup>R</sup>	This study
$\Delta$ fadD23	<i>M. smegmatis</i> mc <sup>2</sup> 155 $\Delta$ fadD23::ZeoR	Ref. 36 <sup>5</sup>
$\Delta$ papA3	<i>M. smegmatis</i> mc <sup>2</sup> 155 $\Delta$ papA3::ZeoR	Ref. 36 <sup>5</sup>
GD273	<i>M. abscessus subsp. massiliense</i>	This study
GD286	<i>M. abscessus subsp. massiliense</i>	This study
$\Delta$ papA3 :pLA155	<i>M. smegmatis</i> mc <sup>2</sup> 155 $\Delta$ fadD23 containing vector pLA155	This study
$\Delta$ papA3 :pKSW131	<i>M. smegmatis</i> mc <sup>2</sup> 155 $\Delta$ papA3 complemented with pKSW131	This study

<sup>1</sup>Data from reference 54. <sup>2</sup>Data from reference 24. <sup>3</sup>Data from reference 4. <sup>4</sup>Data from reference 9. <sup>5</sup>Data from reference 36.

## Extended Data Table 5 | Plasmids and primers used in this study

Name	Plasmid/Primer	Description
pMV <i>pks_mWasabi</i>	Plasmid	pMV361eH containing <i>pks</i> under the control of its own promoter <sup>1</sup> and <i>mWasabi</i> sequence under the control of the constitutive <i>Pleft*</i> promoter (addgene plasmid :169409)
pMV <i>mmpL10_mWasabi</i>	Plasmid	pMV361eH containing <i>mmpL10</i> under the control of the <i>PblaF*</i> promoter <sup>1</sup> and <i>mWasabi</i> sequence under the control of the constitutive <i>Pleft*</i> promoter (addgene plasmid :169409)
pLA155	Plasmid	pMH94 (L5 integrase) where the Kanamycin resistance cassette has been replaced with a streptomycin resistance cassette
pKSW131	Plasmid	pLA155 containing <i>papA3</i> , <i>mmpL10</i> , <i>pE</i> and <i>fadD23</i> from <i>M. abscessus</i> GD01 under control of the native promoter
pKSW134	Plasmid	pCCK39 (L5 integrase, streptomycin resistance cassette) containing <i>fadD23</i> from <i>M. abscessus</i> GD01 under control of a tet-inducible promoter.
Inf_ <i>Pleft*_mWasabi_pMV</i> (KpnI) (F)	Primer	5'-CCACTGCGATCCCCGGGTACTGATGCCTGGCAGTCGATCGT
Inf_ <i>Pleft*_mWasabi_pMV</i> (KpnI) (R)	Primer	5'-CGTCGCCGAGGGCTTGGTACGGCCGCGGTACCAGATCTT
TPP_pMH94_Fwd	Primer	5'-TTGTAAAACGACGGCCAGTGAATTCTTGTGGCCTCCTTGCGTC
TPP_pMH94_Rev	Primer	5'-ATCCCCGGGTACCGAGCTCGAATTCACCGAGAGGCTAGGCGAC
FadD_pCCK39_Fwd	Primer	5'- GATTCGCCGCCCGAAATCACAGCGTGACTTGGACAAAACCTATGACACC
FadD-pCCK39_Rev	Primer	5'-GCGTTTAAACCTGCAGGCACCTAGGCGACGCCACCGG

## Reporting Summary

Nature Portfolio wishes to improve the reproducibility of the work that we publish. This form provides structure for consistency and transparency in reporting. For further information on Nature Portfolio policies, see our [Editorial Policies](#) and the [Editorial Policy Checklist](#).

### Statistics

For all statistical analyses, confirm that the following items are present in the figure legend, table legend, main text, or Methods section.

- | n/a                                 | Confirmed  |
|-------------------------------------|--|
| <input type="checkbox"/>            | <input checked="" type="checkbox"/> The exact sample size ( $n$ ) for each experimental group/condition, given as a discrete number and unit of measurement  |
| <input checked="" type="checkbox"/> | <input type="checkbox"/> A statement on whether measurements were taken from distinct samples or whether the same sample was measured repeatedly   |
| <input type="checkbox"/>            | <input checked="" type="checkbox"/> The statistical test(s) used AND whether they are one- or two-sided<br><i>Only common tests should be described solely by name; describe more complex techniques in the Methods section.</i>   |
| <input checked="" type="checkbox"/> | <input type="checkbox"/> A description of all covariates tested  |
| <input checked="" type="checkbox"/> | <input type="checkbox"/> A description of any assumptions or corrections, such as tests of normality and adjustment for multiple comparisons   |
| <input type="checkbox"/>            | <input checked="" type="checkbox"/> A full description of the statistical parameters including central tendency (e.g. means) or other basic estimates (e.g. regression coefficient) AND variation (e.g. standard deviation) or associated estimates of uncertainty (e.g. confidence intervals) |
| <input type="checkbox"/>            | <input checked="" type="checkbox"/> For null hypothesis testing, the test statistic (e.g. $F$ , $t$ , $r$ ) with confidence intervals, effect sizes, degrees of freedom and $P$ value noted<br><i>Give <math>P</math> values as exact values whenever suitable.</i>                            |
| <input checked="" type="checkbox"/> | <input type="checkbox"/> For Bayesian analysis, information on the choice of priors and Markov chain Monte Carlo settings  |
| <input checked="" type="checkbox"/> | <input type="checkbox"/> For hierarchical and complex designs, identification of the appropriate level for tests and full reporting of outcomes  |
| <input checked="" type="checkbox"/> | <input type="checkbox"/> Estimates of effect sizes (e.g. Cohen's $d$ , Pearson's $r$ ), indicating how they were calculated  |

*Our web collection on [statistics for biologists](#) contains articles on many of the points above.*

### Software and code

Policy information about [availability of computer code](#)

Data collection Flow cytometry data was collected with NovoExpress.

Data analysis Flow cytometry data was analyzed with NovoExpress. Fluorescent images were analyzed with Fiji. Graphs were generated and infection/adsorption data analyzed with GraphPad Prism 9.0. M. abscessus strain sequences were analyzed using MMSeqs2 (v13.45111), phammseqs (v1.0.4), ClustalO (v1.2.4), Trimal (v1.4.1) and RAXML (v8.2.12). The concatenated amino acid alignment was generated with a custom Python script.

For manuscripts utilizing custom algorithms or software that are central to the research but not yet described in published literature, software must be made available to editors and reviewers. We strongly encourage code deposition in a community repository (e.g. GitHub). See the Nature Portfolio [guidelines for submitting code & software](#) for further information.

## Data

Policy information about [availability of data](#)

All manuscripts must include a [data availability statement](#). This statement should provide the following information, where applicable:

- Accession codes, unique identifiers, or web links for publicly available datasets
- A description of any restrictions on data availability
- For clinical datasets or third party data, please ensure that the statement adheres to our [policy](#)

Sequences of newly reported M. abscessus isolates are deposited in GenBank (accession numbers pending). All phage sequences are publicly available (phagesdb.org).

## Human research participants

Policy information about [studies involving human research participants and Sex and Gender in Research](#).

Reporting on sex and gender	N/A
Population characteristics	N/A
Recruitment	N/A
Ethics oversight	N/A

Note that full information on the approval of the study protocol must also be provided in the manuscript.

## Field-specific reporting

Please select the one below that is the best fit for your research. If you are not sure, read the appropriate sections before making your selection.

Life sciences       Behavioural & social sciences       Ecological, evolutionary & environmental sciences

For a reference copy of the document with all sections, see [nature.com/documents/nr-reporting-summary-flat.pdf](https://www.nature.com/documents/nr-reporting-summary-flat.pdf)

## Life sciences study design

All studies must disclose on these points even when the disclosure is negative.

Sample size	N/A
Data exclusions	No data exclusions.
Replication	All experiments that measured various steps in phage infection were performed in duplicate or triplicate, and performed at least twice. Similar results were found every time.
Randomization	N/A
Blinding	N/A

## Reporting for specific materials, systems and methods

We require information from authors about some types of materials, experimental systems and methods used in many studies. Here, indicate whether each material, system or method listed is relevant to your study. If you are not sure if a list item applies to your research, read the appropriate section before selecting a response.

## Materials &amp; experimental systems

- n/a | Involved in the study
- Antibodies
- Eukaryotic cell lines
- Palaeontology and archaeology
- Animals and other organisms
- Clinical data
- Dual use research of concern

## Methods

- n/a | Involved in the study
- ChIP-seq
- Flow cytometry
- MRI-based neuroimaging

## Flow Cytometry

## Plots

Confirm that:

- The axis labels state the marker and fluorochrome used (e.g. CD4-FITC).
- The axis scales are clearly visible. Include numbers along axes only for bottom left plot of group (a 'group' is an analysis of identical markers).
- All plots are contour plots with outliers or pseudocolor plots.
- A numerical value for number of cells or percentage (with statistics) is provided.

## Methodology

Sample preparation

M. abscessus or M. smegmatis cells were incubated with either medium or phage BPs\_Δ33HTH\_HRM10 as controls or phage BPs\_Δ33HTH\_HRM10 mCherry (MOI 10). After incubation, samples were fixed with PFA 4% for 20 min at room temperature. Samples were then diluted as necessary depending on the experiment with 7H9/OADC supplemented with 0.025% tyloxapol and sonicated to disrupt bacterial aggregates.

Instrument

NovoCyte ACEA flow cytometer

Software

NovoExpress

Cell population abundance

Approximately 300,000 events were recorded per experiment.

Gating strategy

Gates were drawn using SSC-A/FSC-A and multiples of cells were excluded with SSC-H / SSC-A.

- Tick this box to confirm that a figure exemplifying the gating strategy is provided in the Supplementary Information.